PROTONS IN FLARES

G. M. SIMNETT
School of Physics and Space Research, University of Birmingham, B15 2TT, UK

(Received 3 February, 1995)

Abstract. This work addresses the role of non-thermal protons as a means of transporting energy in stellar atmospheres. The most dramatic transient visible phenomena are flares, the best studied of which are from the Sun. It is believed that energetic particles take a fundamental part in flare development, but it is controversial as to whether protons or electrons play the dominant role. This review is aimed at helping resolve the controversy. We start by outlining acceleration mechanisms for energetic particles, on the premise that the acceleration site is in the corona. The propagation of a proton beam through the atmosphere is discussed, together with the radiation signatures it would produce. Chromospheric evaporation is expected as the beam reaches the dense part of the atmosphere. Direct observational evidence for energetic protons is reviewed, from gamma-ray production involving energies > 30 MeV to Hα polarization, which is significant at energies $\lesssim 100$ keV. Proton beams can be detected in the corona via slowly-drifting type III bursts, while they can be directly sampled by spacecraft and, at energies > 1 GeV, by detectors on the Earth. A number of key flare observations and energy arguments are debated from the viewpoint of protons versus electrons. The conclusion is that primary non-thermal protons are much more important, in terms of total energy, than non-thermal electrons in flares, and that the bulk of the energetic electrons are secondary.

1. Introduction

Despite a wealth of high quality, high resolution data, there still remain significant unanswered questions regarding the precise physical processes responsible for a solar or stellar flare. This review examines how non-thermal protons might provide some solutions and we adopt the following format: an introduction to the problem; how do we accelerate non-thermal protons (and electrons); what do we *expect* to see; what *do* we see; how do we reconcile observations with expectations; what implications are there for phenomena other than flares; and where should we go next?

The interest in the role of protons in solar and stellar flares stems from the need to account for the impulsive events which accompany the sudden brightening we call a flare. The proton is of interest in a broader context on account of its ability to carry energy and momentum, without radiating significantly, over large distances (actually integrated column density). Their energy losses/unit distance/unit time are very predictable. Protons are almost invisible. Only at high energies, certainly well beyond the part of the spectrum where most of the energy resides, do protons become easily 'visible'. These properties are not shared by electrons as not only do they radiate profusely but they are very easily scattered; also, on account of their high velocity/unit energy, in the same environment as the proton they traverse much more matter/unit time for the same energy.

Space Science Reviews **73:** 387–432, 1995.

In large solar flares the impulsive phase emissions occur almost simultaneously over a wide spectral range, certainly from cm wavelengths ($h\nu \sim 10^{-4}$ eV) to 100 MeV gamma-rays – a range of at least 10^{12}. Gamma-rays are seen relatively rarely. Electrons have attracted most attention as the cause of the radiation simply because of their radiative properties. Strictly speaking, rightly so, as most of the radiation comes immediately from electrons (e.g., before the energy was in the photon it was carried by an electron). However, this picture may be too simplistic and the question has been raised as to whether, after all, the majority of the energetic electrons might be secondary. To help answer this question we need to evaluate the role of protons in flares.

The optical emissions are easiest to detect and these are studied with high spatial and spectral resolution. They originate from deep in the atmosphere (hydrogen density $> 10^{14}$ cm^{-3}) and one of our first tasks is to decide if this is actually where (or close to) the primary energy release takes place, or whether it is merely a dumping ground? To set this question in context, we start with one of the few points the community is agreed on, namely that the flare energy comes from the non-potential magnetic field associated with currents in the atmosphere (Giovanelli, 1947; Dungey, 1953; Sweet, 1969). In a volume V, when the magnetic field changes from an initial value B_i to a final value B_f, the energy released is $(B_i^2 - B_f^2)V/8\pi$. In a very large solar flare this must be $\sim 10^{32}$ erg; in stellar flares this could be $> 10^{35}$ erg (Roizman and Shevchenko, 1982); and Peterson (1989) has suggested that it might occasionally be as high as 10^{37} erg. Clearly there is an advantage to extracting this energy from a large change in B, over a small volume, than *vice versa*. However, the time scale is awkward, as classical dissipation processes lead to energy release times $\gg 10^2$–10^3 s required to account for flares. Strong fields are relatively easy to measure, but it has never been possible to show consistently that the magnetic field change within an active region could account for the observed energy release. Some promising acceleration mechanisms require extensive current sheets in order to produce protons of 20 GeV, the extreme energy required occasionally. This points to the corona as the reconnection region. This is convenient from a theorist's viewpoint, as coronal magnetic fields are difficult to measure!

There is a further consideration. Hoyng *et al.* (1976) argued that the impulsive phase of a large flare required 10^{36} electrons s^{-1} above 25 keV to account for the hard X-ray burst, assuming that it was produced classically by electron-ion bremsstrahlung. If the impulsive phase lasts 10^3s, 10^{39} electrons are needed; at a mean energy of 25 keV this is 4×10^{31} erg. This is the total number of electrons in a cube of side 10^5 km at a mean density of 10^9 cm^{-3}. Murphy *et al.* (1993) calculated the number of protons > 30 MeV in a recent γ-ray flare as $> 1.5 \times 10^{33}$. In the flare they studied they deduced a differential energy number spectrum for the protons given by:

$$\mathrm{d}J/\mathrm{d}E \propto E^{-\gamma} \tag{1}$$

with $\gamma = 2.8$. If this spectrum continues towards lower energies, the number of protons above 300 keV is 10^{37}, with a total energy of 10^{31} erg. If the spectrum continues to rise appreciably to even lower energies, the total energy goes up even higher. It is clear that protons can, and would, be a major contribution to the energy budget and that the total number of source particles may be over an order-of-magnitude less than for the primary electron case. In a scenario that is already straining the bounds of credibility, a reduction of this magnitude in the sheer amount of material to be energised is welcome, although not proven. The location of the energy release site is still an open question, but for the purpose of the subsequent discussion it is assumed to be in the corona.

The other main question is whether the bulk of the energy is transferred by protons, or electrons, or is it transferred another way and the observed protons and electrons are merely secondary? In considering the energy budget we must be very careful to avoid double accounting. If we deduce $\sim 10^{31}$ ergs from X-ray emitting electrons, and $\sim 10^{31}$ ergs from gamma-ray-producing protons, how certain are we that one is not a secondary product of the other? Could an explosively-heated plasma subsequently form shock waves that accelerate both electrons and protons? These questions may be sharpened by the fact that the impulsive phase hard X-ray burst, which is undoubtedly when the energy content of the non-thermal electrons is highest, generally precedes the maximum development of the hot thermal plasma. Therefore it is unlikely, from a causality argument, that the bulk of the energetic particles are secondary to the energy in the plasma.

It has been claimed (Colgate, 1978; Simnett, 1986) that big flares cannot be powered by non-thermal electrons. Colgate argued from theoretical grounds, while Simnett relied more on causality arguments based on the observations. It is important for the community to reach a consensus for the following reasons:

(1) The particle acceleration mechanism could probably be decided if the required output was known.

(2) The acceleration mechanism will probably indicate where in the atmosphere conditions are appropriate for it to operate.

(3) Resolution of (1) and (2) will have a profound theoretical input to the problems of understanding the coronal magnetic field, coronal heating, coronal mass ejections and the origin of the solar wind.

Not all these questions will be answered, or even addressed, here. Section 2 concentrates on proton acceleration mechanisms, Section 3 covers proton propagation through the atmosphere, and what happens when they stop (chromospheric evaporation). Section 4 reviews the available evidence that non-thermal protons are present in the solar (stellar) atmosphere at certain times. Section 5 discusses some key observations, focusing on the support they offer the non-thermal proton model. If proton acceleration is taking place in large structures in the corona, then we might reasonably expect the effects to be more global than simply a flare in an active region. In some nearby dMe stars, flares are easily visible in the optical band against the full stellar background, consistent with a global effect. In recognition of

this, in Section 6 we take two currently unexplained phenomena, explosive events in the transition zone and the triggering of coronal mass ejections, and examine how they might be accounted for by the presence of non-thermal protons.

2. Particle Acceleration Mechanisms

2.1. Proton acceleration

Particle acceleration in solar flares has been studied theoretically for several decades. Wentzel (1965) appealed to the Fermi mechanism to account for the relativistic ions observed in ground level events, where the energy of the particles can be deduced from a combination of the atmospheric transmission and the geomagnetic cut-off rigidity at the observing site. Therefore although the Fermi mechanism as considered by Wentzel could accelerate particles to high energies, it takes too long to be useful in explaining all the current observations. One difficulty facing the theorists is to identify the precise problem to be tackled. There are many facets to this: the highest energy to be accelerated; the speed of the acceleration; the energy spectrum; the composition of the accelerated particles, not only elemental but isotopic; the electron/proton ratio, etc.

Different workers have addressed different aspects of the acceleration question, depending on which parameters of the flare they were focusing on. As of this date a comprehensive model has yet to emerge, although if electron acceleration could be decoupled from proton acceleration we might be a lot closer! The most appealing goal is to come up with a simple physical mechanism whereby simple scaling of some basic parameters, e.g., size, magnetic field strength, number density, and temperature, would naturally account for differences from event to event. The most elegant early attempt at this solution was the circuit theory model (Alfvén and Carlqvist, 1967) which, by virtue of interrupting the current responsible for the non-potential field can, in principle, provide a large accelerating field to energise the particles. In practice this ran into difficulties in that the inductance is high and the resistance is low, leading to apparently insurmountable problems. Melrose and McClymont (1987) appealed to electron collisions with the ion-sound turbulence to provide increased (anomalous) resistivity, but only after invoking extreme filamentation of the current in a coronal loop to provide a filling factor of $\sim 10^{-5}$. Zaitsev and Stepanov (1992) recently argued that the ion-neutral atom collisions in the energy release volume might be the solution to the rapid energy dissipation problem; however, the model cannot explain the high proton energies observed in many flares.

Shock acceleration has received considerable attention, partly because there are plausible ways of accelerating ions out of a thermal population (Chiueh, 1988), which may then be used as an input to shock acceleration mechanisms which require a threshold energy for injection (Decker and Vlahos, 1986). The results of Decker

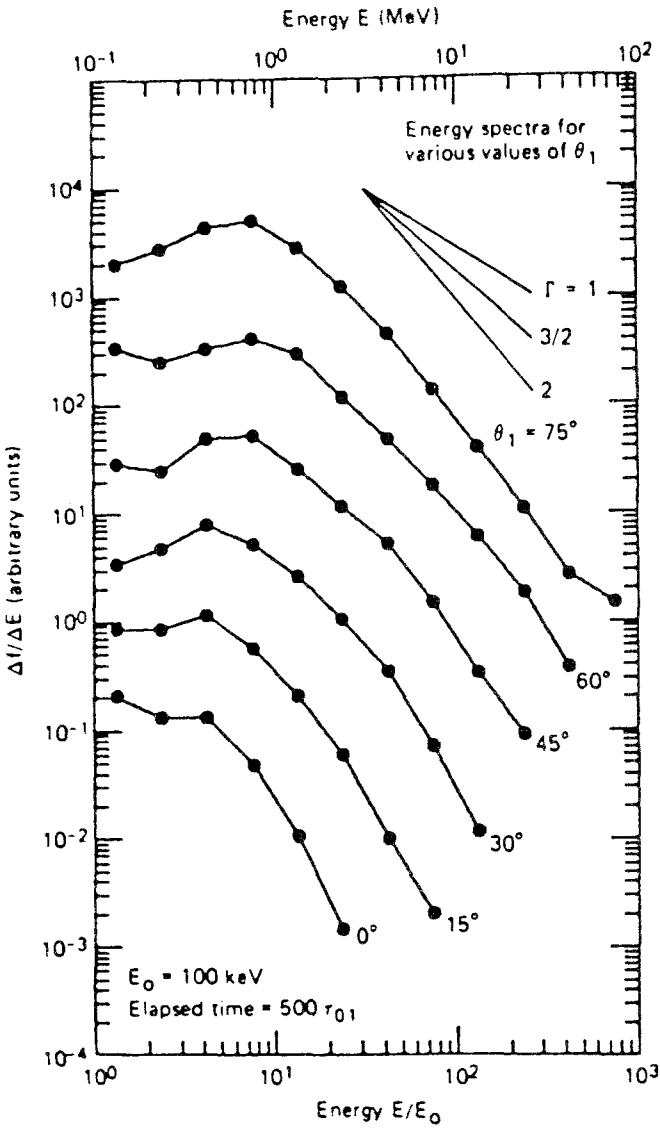

Fig. 1. Predicted proton energy spectra from acceleration at turbulent shocks. θ is the angle the upstream magnetic field makes to the shock normal. The proton injection energy is 100 keV. τ_{01} is the proton upstream gyroperiod. Spectra of various slopes are indicated in the upper right of the figure. (After Decker and Vlahos, 1986.)

and Vlahos are shown in Figure 1 for acceleration in a turbulent, oblique shock. A combination of Chiueh's mechanism and that of Decker and Vlahos is attractive for the following reason. Initially there may be negligible upstream turbulence to scatter the particles. As the acceleration proceeds, upstream scattering is produced through Alfvén wave turbulence, where the Alfvén waves are generated by the accelerated ions themselves.

Ohsawa (1985) realised that a resonance phenomenon associated with fast, magnetosonic shock waves could accelerate rapidly some fraction of the particle population to high, even relativistic, energies. For protons, the final velocity, v, is given by

$$v = v_{\mathrm{A}} \left(\frac{m_p}{m_e}\right)^{1/2} (M_{\mathrm{A}} - 1)^{3/2} , \tag{2}$$

where v_{A} is the Alfvén velocity; m_p, m_e the proton and electron masses; and M_{A} is the Mach number of the shock. This process is reviewed comprehensively by Sakai and Ohsawa (1987). In a shock propagating in the inner heliosphere, where the Alfvén speed may be a few $\times 10^2$ km s^{-1}, the maximum energy is in the region of 1–10 MeV, which is consistent with *in situ* observations. In the very low corona, if the magnetic field is 10^3 G, such that the proton cyclotron frequency $\omega_{ci} \gtrsim$ plasma frequency, then acceleration to relativistic energies will occur in time scales of $(m_p/m_e)^{1/2}\omega_{ci}^{-1} \lesssim 1$ s. Again, one could argue that this is consistent with gamma-ray observations at times of flares (Section 3). Unlike classical Fermi acceleration, where the energy gain is slow, shock acceleration mechanisms may act rapidly as the process is related to the cyclotron frequency. Decker and Vlahos (1986) could produce 50 MeV protons from an injection energy of 0.1 MeV in < 10 ms, in a magnetic field of 5 G.

Other promising proton acceleration mechanisms involve some kind of direct electric field acceleration such as those proposed by Speiser (1965) and Sakai *et al.* (1987). Speiser's mechanism involves acceleration of both protons and electrons in a current sheet, such as would be produced by magnetic field reconnection. The kinetic energy gain is

$$\Delta T = 2m(E/B_p)^2 , \tag{3}$$

where E is the accelerating electric field and B_p is the (small) component of the magnetic field perpendicular to the current sheet. Martens (1988) has applied Speiser's model, which was originally proposed to account for proton acceleration in the geomagnetic tail, to the solar corona. For realistic coronal parameters Martens predicted a proton spectrum from 100 keV–20 GeV. The upper limit comes from taking the observed electric fields of $\sim$ 2 V cm^{-1} in the current sheet above two ribbon flares (Kopp and Poletto, 1986; Foukal *et al.*, 1987) and the observed length, 2×10^{10} cm, of the associated pre-flare filament. During the eruptive phase the reconnection is driven harder and Foukal *et al.* have reported upper limits of 5–10 V cm^{-1} from analysing Stark broadening of emission lines. For strong reconnection Kopp and Poletto calculate fields of > 10 V cm^{-1}. It is interesting to note that the upper limit calculated by Martens (1988) is close to that observed in the rare, very energetic solar events.

Martens (1988) addressed the important question of the supply of material to be accelerated. The $\mathbf{E} \times \mathbf{B}$ force causes plasma to drift into the current sheet and

for an ambient density of 10^{10} cm^{-3} and a magnetic field of 100 G he calculates a supply of protons of 4×10^{35} s^{-1}. Martens and Young (1990) have developed these ideas further and they point out that the electric field is five orders of magnitude more than the Dreicer field in the corona. They calculate the effective resistivity to be 3×10^6 times the classical collisional Spitzer resistivity. It is likely that the energy release process is totally governed by the amount of material present. The energy extracted from the field goes at the maximum rate permitted by the supply of material, as this governs the effective resistivity. Therefore we expect 100% of the plasma in the reconnection region to be accelerated. Material supply to the corona may in fact be the controlling factor in understanding energetic transient solar phenomena.

Simnett (1991a) has reviewed the main published ion acceleration mechanisms and the reader is referred to this work for detailed comparison of them, plus references to previous reviews on the subject. One thing that most of these mechanisms have in common is that, on an energy/particle basis, they accelerate ions (protons) rather than electrons. The Speiser (1965) mechanism accelerates electrons and ions to equal velocities; Chiueh's (1988) mechanism does not accelerate electrons significantly; the explosive coalescence mechanism of Sakai *et al.* (1986) accelerates electrons relative to protons approximately as $(m_e/m_p)^{1/2}$. These predictions are broadly consistent with the experience we have (a) from observations of γ-ray production in flares and (b) from direct detection of energetic flare particles in the interplanetary medium. For the 21 June, 1980 gamma-ray flare the e/p ratio above 30 MeV was a 1.5×10^{-2} (Ramaty and Murphy, 1987), while Evanson *et al.* (1984) showed from interplanetary particle measurements that this ratio for flares without gamma-ray emission could be several orders of magnitude lower, consistent with the first measurements of this ratio (Datlowe, 1971). Therefore the definitive observations strongly support a number of theoretical results from particle acceleration mechanisms.

2.2. Electron Acceleration

It is worth mentioning briefly proposals for electron acceleration. These models are deliberately aimed at producing electrons without a significant fraction of the energy in accompanying ions, driven by the belief that only electrons are important, energetically, in the early phase of flares. An early attempt (Hoyng, 1977; Hoyng *et al.*, 1980) invoked acceleration by Langmuir waves, but could not produce electrons above $\sim$ 50 keV. Smith (1985) considered a modified two-stream (electron, ion) instability where electrons could also reach $\sim$ 50 keV, but he estimated that no more than 23% of the energy could go into streaming electrons.

Holman (1985) attempted to alleviate the problem of the large number of energetic electrons required by supposing that the bulk of the electrons responsible for the hard X-ray burst were thermal, and that some electrons in the high-energy tail of the thermal distribution were able to experience run-away acceleration in the

quasi-static DC electric fields set up parallel to the magnetic field in the current sheet. More recently, LaRosa and Moore (1993) have discussed bulk energization of all the electrons in a large volume of the solar atmosphere by an MHD turbulent cascade, resulting from the output of a large number of separate magnetic reconnections. One difficulty was preventing the escape of the electrons before they had reached a high energy and they supposed the turbulence in the magnetic field would achieve this. Other problems are that the model would not predict a low energy cut-off in the electron distribution which is required, from energetics considerations, from interpretation of the hard X-ray burst; and it did not appear to be able to achieve energies much higher than 25 keV. Further work (LaRosa *et al.*, 1994) identified the physical mechanism responsible for the electron energisation as Fermi acceleration, and they regarded the lack of acceleration of ions by their model as an advantage!

The above proposals are focused on obtaining a large number of electrons > 25 keV which are needed to explain the hard X-ray burst. The models are not very successful in generating electrons in the 10^2 keV or MeV regions of the spectrum. The outcome of this is at best unsatisfactory at accounting for all aspects of the observations.

2.3. Electron Acceleration as a Secondary Process

In recognition of two main facts: (1) that most theoretical particle acceleration processes relevant to solar flares accelerate protons very much better than electrons and (2) that during the impulsive phase of flares there is *apparently* more energy in non-thermal electrons than in other particles, Simnett and Haines (1990) proposed that the non-thermal electrons were secondary to the primary particle acceleration process. The essential ingredient of their model is that a neutralized ion (proton) and electron beam, with no net current, is accelerated by a process (see Section 2.1) resulting from magnetic reconnection in the corona. The beam propagates along the local magnetic field towards the chromosphere where it encounters the density discontinuity at the top of the transition region (see Figure 3, Section 3). At this level the beam electrons, which have the same velocity as the ions, scatter and effectively stop. The protons, with their larger momentum, continue. The situation is illustrated schematically in Figure 2. Because the electrons stop and the protons continue, an electric double layer will be established unless some way is found to neutralize it. For low beam fluxes there is an ample supply of cold, chromospheric electrons to achieve this. However, if the beam flux is large enough, the resistivity of the chromosphere is too high to supply sufficient electrons fast enough. In this situation a potential, Φ, develops in the transition region which accelerates the highest energy electrons available, namely those in the beam which have higher than average velocities.

For a test situation with a beam of 1 MeV protons and 500 eV electrons Simnett and Haines found that (a) the electric field developed exceeded the Dreicer field

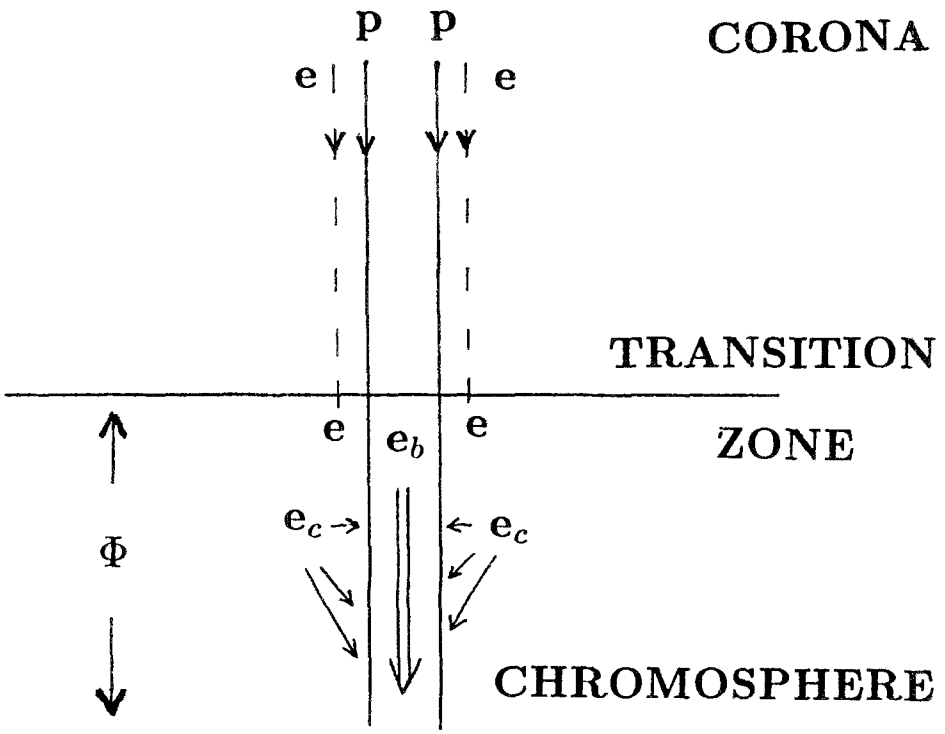

Fig. 2. The concept of the development of an electric potential Φ below the transition zone which may lead to runaway electron acceleration using the Simnett and Haines (1990) model. With this model a neutral beam of ions and electrons is incident on the transition zone from the corona. For low beam fluxes the potential is neutralised by cold chromospheric electrons, e_c. Above a certain flux threshold the resistivity of the chromosphere is too high for effective neutralisation to occur, and beam electrons e_b experience runaway acceleration. (After Simnett, 1991a.)

and (b) the condition for acceleration was achieved when the ratio of the beam density to the local plasma density was significantly above 10^{-3}.

The Simnett and Haines concept has a number of attractive features which are consistent with observations discussed in Sections 4 and 5. These include active region pre-heating, early onset of chromospheric evaporation, delay of the microwave radio emission with respect to correlated X-ray emission, arbitrary phase of the hard X-ray production with respect to the plasma heating, and energy balance. Brown (1991) has criticised the model in that it does not alleviate the main problem it is designed to solve, namely the energy in the electron population. However, it does achieve this in the following ways:

(1) The non-thermal electrons are all runaways, so there is no need to invoke any part of the distribution at low energies, where, with a power-law number/energy distribution with $\gamma > 2$, most of the energy resides.

(2) The plasma is already pre-heated by Coulomb losses of the beam before the runaway electron acceleration condition is reached. Therefore the non-thermal

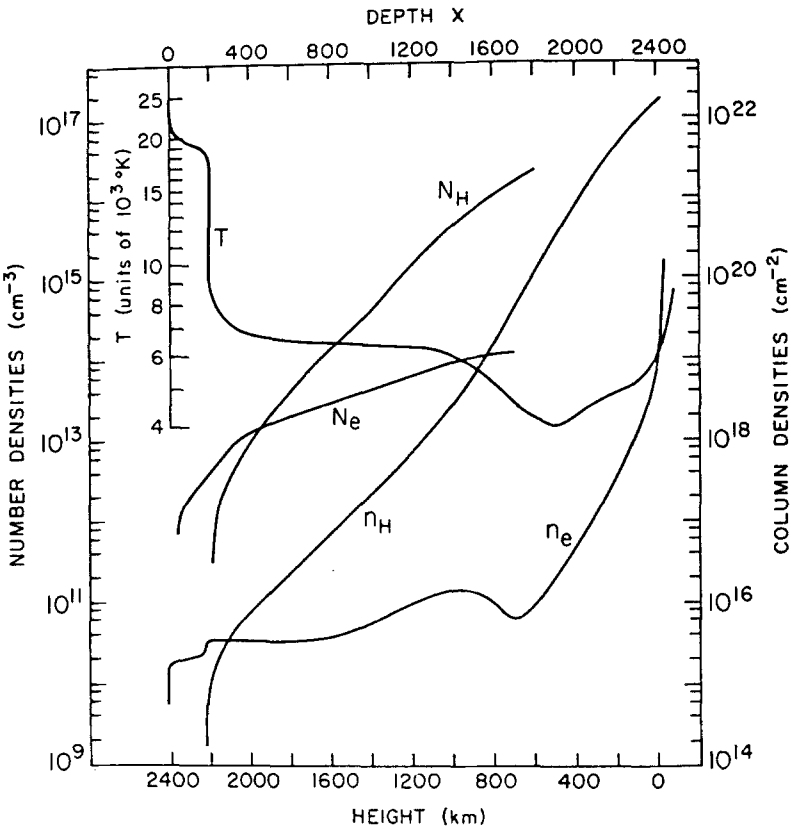

Fig. 3. The height dependence of the temperature T, electron density n_e, and neutral hydrogen density n_H above the photosphere. Also shown are the column densities of electrons (N_e) and neutral hydrogen (N_H) below the transition zone (upper and right scales). (After Orrall and Zirker, 1976.)

electron bremsstrahlung is in a very hot target, which makes the electrons more efficient for hard X-ray production. Also the Dreicer field is inversely proportional to the plasma electron temperature, which makes runaway acceleration easier in a hot target.

(3) The electrons are totally secondary to the protons. Therefore the energy in the electron population is not added to the ion energy budget. If the energy input into protons from the primary reconnection is $W(t)$, then the total energy given to the protons, which is the total flare energy, is

$$W_p = \int_0^{t_f} W(t)\,\mathrm{d}t\,, \tag{4}$$

where t_f is the time corresponding to the end of the energy release, which is assumed to start at $t = 0$. If the times corresponding to the onset and end of the impulsive non-thermal hard X-ray burst are t_{x1} and t_{x2}, respectively, which cover

the period when the runaway electron acceleration condition is satisfied, then the energy given to the non-thermal electrons is

$$E_{nte} = \int_{t_{x1}}^{t_{x2}} \epsilon(t) W(t)\, \mathrm{d}t\ , \tag{5}$$

where $\epsilon(t)$ is the efficiency with which the ion energy is transferred to the electrons provided the runaway condition is satisfied. Simnett and Haines (1990) showed that $\epsilon(t)$ could easily be > 0.9. In practice filamentation of the beam may occur (Winglee *et al.*, 1988; Benz, 1985) such that in the chromosphere i separate filaments may participate in the flare, each independently producing electron acceleration. Therefore Equation (4) would be modified such that the energy in the non-thermal electrons is

$$E_{nte} = \sum_i \int_{t_{x1i}}^{t_{x2i}} \epsilon_i(t) W(t)\, \mathrm{d}t\ , \tag{6}$$

where t_{x1i} and t_{x2i} are the start and stop times for the runaway condition in the ith filament. This idea is virtually identical to the proposal by de Jager and de Jonge (1978) that flares are simply a collection of elementary flare bursts.

(4) With a proton beam the typical energy/particle may be $\sim$ 0.5 MeV; if the typical energy in a hypothetical electron beam is 25 keV, then a factor of 20 fewer particles are needed to transport the same amount of energy. As discussed by LaRosa and Moore (1993), and others, the total number of particles required to provide flare energies of 10^{32} erg is a problem; any mechanism that has the potential of reducing this number by an order-of-magnitude is welcome.

3. Proton Beam Propagation through the Atmosphere

3.1. CHARGE EXCHANGE

Orrall and Zirker (1976) were the first to make detailed calculations on the propagation of protons through the atmosphere. They investigated the interaction of protons of energies 10 keV–1 MeV with chromospheric hydrogen atoms. They primarily considered stopping due to ionization of the atoms, i.e., interactions with the bound electrons, but they also considered the effect of free electrons in recognition of the fact that the atmosphere is partially ionized. The main thrust of their work was to calculate the production of fast neutral atoms by charge exchange with the proton beam as it slowed down. They used the atmospheric model of Vernazza *et al.* (1973), which is reproduced in Figure 3. Here is plotted the temperature T, electron density n_e and the neutral hydrogen density n_{H} as a function of height

above the photosphere. Also shown (upper and right scales) are the column densities of electrons, N_e, and neutral hydrogen atoms, N_H, as a function of depth below the transition zone, taken to be 2400 km above the photosphere. They used these curves to calculate the height at which the protons are stopped through interactions with electrons and neutral hydrogen.

Using the cross-sections for the production of the relevant excited state of hydrogen they calculated the expected Lα profile in the atmosphere as a function of the spectrum of the incident proton beam. With a modest energy flux of 2×10^7 erg cm^{-2} s^{-1} they predicted a detectable asymmetry (towards the red-wing) in the Lα profile. For typical power-law proton spectra the dominant contribution to the asymmetry was from protons in the 20–30 keV range.

These calculations were extended by Canfield and Chang (1985) to include the production of both Lα and Hα. They found that the Lα red-wing intensity was orders of magnitude larger than observed active region or flare values, but that the Hα red-wing intensity was somewhat less than a typical active region value. In terms of stopping the beam, which is relevant to the depth at which the majority of the Lα is produced, they considered only collisions with electrons. They calculated the line profile for a wide range of different possible energy spectra, but in all cases the peak Lα red-wing intensity occurred around 10 Å from the line centre.

A very comprehensive treatment of this problem has recently been performed by Brosius *et al.* (1994). They considered interactions with neutral hydrogen atoms, including interactions of the beam protons with the nuclei, and with the background plasma, both protons and electrons. They did not take into account the elemental composition of either the atmosphere or the particle beam. Table I shows their beam stopping parameters for various model chromospheres. For simplicity slab atmospheres of thickness d were chosen, with varying degrees of ionization – 10%, 50%, and 90%. The column density under which the protons will stop is shown in the final column of Table I, and this may be compared with the curves in Figure 3. It may be seen that protons of 100 keV are stopped at column densities between 2.6 and 9.4×10^{18} cm^{-2}, depending on the degree of ionization.

The important new point developed by Brosius *et al.* (1994) is that in response to energy input a stellar chromosphere will evolve rapidly in both temperature and ionization state, and it will evolve somewhat in pressure. This means that the energy transfer processes are rapidly changing. Table I shows that in a 10% ionized atmosphere above 100 keV the dominant energy losses are to the neutral atoms, although as the energy falls the losses to the plasma become the most important. This means that the higher energy particles rapidly increase the level of ionization and the lower energy particles, as they lose most of their energy to the plasma, cause the rise in temperature.

Thus when a beam of particles starts to ionize the chromosphere, not only does the percentage ionization increase rapidly, but the energy loss/unit thickness increases, as the beam loses energy to plasma particles more efficiently than it does to neutral atoms. The beam changes from ionizing neutral atoms to heating

TABLE I

Model chromosphere and beam stopping parameters (after Brosius *et al.*, 1994)

n_e (cm^{-3})	$n_p/(n_p + n_H)$	T (K)	E_0 (eV)	Depth (km)	ΔE_{plas} (keV)	ΔE_{neut} (keV)	$n_p + n_H$ column density cm^{-2}
1×10^{10}	0.1	5726.6	1000	4.402×10^4	238.13	761.86	4.4×10^{20}
			300	5.131×10^3	100.47	199.52	5.1×10^{19}
			100	8.968×10^2	51.48	48.51	9×10^{18}
			30	1.440×10^2	23.64	6.35	1.4×10^{18}
1×10^{11}	0.1	6218.1	1000	4.502×10^3	219.32	780.67	4.5×10^{20}
			300	5.291×10^2	93.95	206.04	5.3×10^{19}
			100	9.427×10^1	49.08	50.91	9.4×10^{18}
			30	1.568×10^1	23.10	6.89	1.6×10^{18}
5×10^{10}	0.5	6585.8	100	3.973×10^2	87.90	12.09	4×10^{18}
9×10^{10}	0.9	7391.1	100	2.606×10^2	98.40	1.59	2.6×10^{19}
5×10^{11}	0.5	7238.3	100	4.397×10^1	86.61	13.38	4.4×10^{18}
9×10^{11}	0.9	8215.6	100	2.933×10^1	98.20	1.79	2.9×10^{18}

the plasma and for a given incident energy, parts of the chromosphere previously reached by the beam will no longer be affected. There will be radiative cooling and recombination in the lower regions which were originally affected by the beam. The most dramatic effect on the radiation signature is that the downward moving protons can no longer reach any neutral hydrogen atoms with which they can charge exchange. Therefore any red-shifted Lα radiation will vanish. This fact alone could explain the null result of Canfield and Cook (1978) who searched the *Skylab* data for the Lα signature. Brosius *et al.* (1994) calculate the time scale over which the signature should disappear for different strength beams. For a weak beam of 10^{14} 100 keV protons cm^{-2} s^{-1} in an atmosphere with electron density $n_e = 10^{10}$ cm^{-3}, the Lα signature turns off after only 10 s, and this reduces to 0.1 s if the flux increases by two orders-of-magnitude. These time scales are only weakly dependent on the initial electron density.

This result has the very curious property that the Lα signature is less observable the stronger the incident beam! It is also interesting that in this context mass motions, which on account of the high ionization state will be along magnetic field lines, can be largely ignored as the beam is stopped at a certain column depth. Mass motions upwards (chromospheric evaporation) merely alter the height at which the beam is stopped, but will not effect the Lα signature.

The conclusion from this study is that the Lα signature should be visible only at the onset of flares when the beam is still weak, or during very small flares. It is clear-

ly an advantage to use spatially resolved observations to reduce the background signal. Although Canfield and Chang (1985) indicated that the signal-to-background was high, their calculations were for an energy flux of 10^{11} erg cm^{-2} s^{-1}, which is so high that the signature should last for less than 0.1 s.

3.2. Hα POLARIZATION

It was realized (Hénoux and Semel, 1981) that observations of Hα polarization can provide evidence of energy transfer to the plasma by beams of particles. They applied the theory of impact polarization of Percival and Seaton (1959) to observations of linear polarization in the Hα line above kernels of flare emission to distinguish between energy transfer via electron bombardment or by heat conduction. The electron impact polarization was a maximum, at 35%, for an excitation energy of 22 eV. Because of scattering the polarization in a flare was unlikely to exceed a few percent. Hénoux *et al.* (1983) argued that the S I line (λ 1436.9 Å) was a better diagnostic than Hα as the polarization levels were higher.

Hénoux and Chambe (1990) realized that in the solar flare situation collisional excitation by proton beams would also produce polarization. The degree of polarization produced by protons is close to that produced by electrons of the same velocity. Hénoux and Chambe recognized that chromospheric flares are usually considered secondary phenomena to coronal energy release and that it was important to distinguish between the following methods of energy transfer: (a) particle beams; (b) X-ray irradiation from a hot coronal source; (c) heat conduction from the same source. These lead to the polarization predictions shown in Figure 4. If the magnetic field guiding the particle beam is vertical, then the electric (E) vector of the collisionally-excited Hα line is perpendicular to the direction from the point of production to disk centre for beam electrons > 20 keV. Photoelectrons from X-ray irradiation produce a polarized fraction opposite to that for an energetic electron beam. However, the velocity distribution of photoelectrons is a maximum in the horizontal plane H, thus giving the same observed polarization direction as for the energetic electron beam. For thermal conduction, the electrons transferring the bulk of the energy have a few times thermal velocity, directed downwards. Collisional excitation by these electrons produces an Hα polarization electric vector towards disk centre.

The example shown in Figure 4 was for electrons, but as mentioned above similar results are expected from protons with similar velocities. In case (a) 20 keV is equivalent to $\sim$ 40 MeV and such protons, if present, are easily detected via gamma-ray line emission. In case (c) the equivalent protons have energy $\sim$ 40 keV and significant polarization is expected up to energies of 200 keV. Therefore observations of linear Hα polarization in the flare to disk-centre direction are a very important diagnostic of low-energy proton beams. Given the constraints on Lα red-wing production discussed in Section 3.1, observations of Hα polarization are

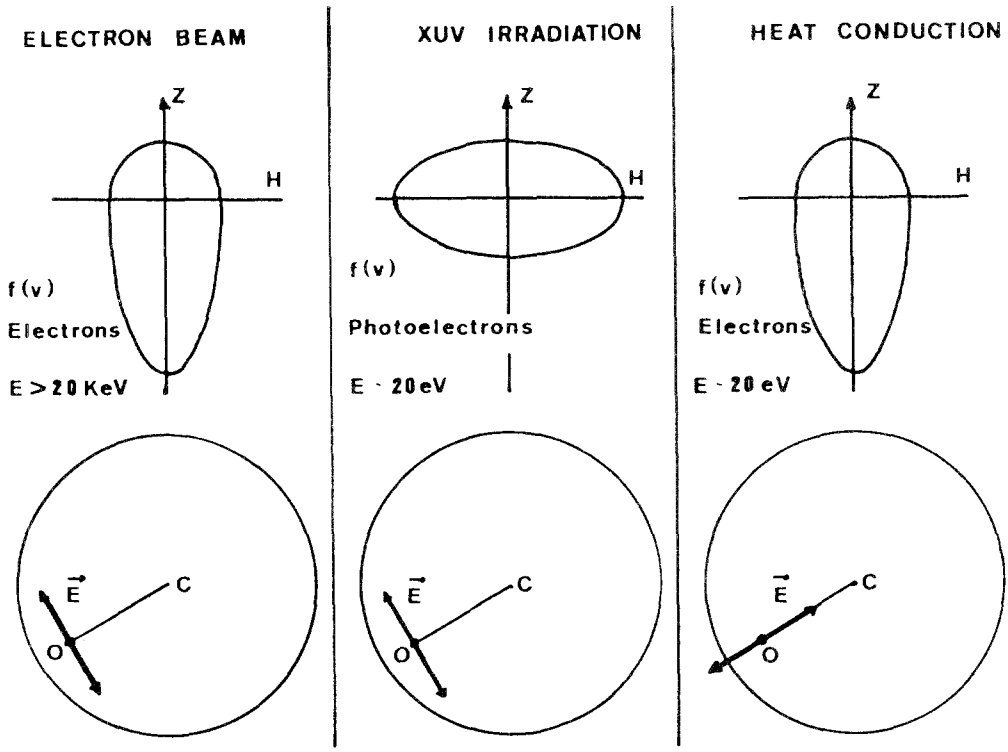

Fig. 4. The direction of vibration of the polarized electric field vector, projected onto the solar disk, for three different energy transport mechanisms. The electron velocity distribution function $f(v)$ is shown in the upper part of the figure for the cases of incident electrons, photoelectrons resulting from XUV irradiation, and thermal electrons. Here Z is the direction of the local vertical and H represents the horizontal. (After Hénoux and Chambe, 1990.)

the best and possibly the only practical way of consistently detecting the presence of protons < 1 MeV in the solar atmosphere.

3.3. GAMMA-RAY PRODUCTION

The most unambiguous signature of energetic protons in the solar atmosphere comes from the variety of neutron and gamma-ray lines produced through nuclear reactions. These processes have been presented in detail by Ramaty *et al.* (1979) and a comprehensive review is given by Ramaty and Murphy (1987). The interaction cross-sections start to become significant at proton (or ion) energies above $\sim$ 10 MeV nucl^{-1}, but it is common to identify strong gamma-ray line flares with protons > 30 MeV. This in part stems from the observation of the neutron capture line at 2.223 MeV; an important source of neutrons is from the break up of ^{4}He nuclei, which have a binding energy $\sim$ 28 MeV. While gamma-ray lines are produced whenever energetic protons are present, the energy content of the part of

the spectrum $> 10-30$ MeV is relatively small compared to the total flare energy. Gamma-rays can tell us little about the presence of protons below ~ 10 MeV.

3.4. CHROMOSPHERIC EVAPORATION AND MASS MOTIONS

The final relevant topic to attract substantial, and diverse, theoretical work is that of mass motions. These may be induced by energy input from either proton or electron beams. The topic covers both chromospheric evaporation and the effect on the atmosphere of momentum deposition. The latter is likely to produce a downward motion which will be observed as a red-shift in an appropriate spectral line. The atmospheric response to rapid energy deposition at a given layer will be to induce a pressure pulse which will drive the overlying material upwards and possibly the underlying material downwards. Therefore there are two possible causes for downward moving material with energy input from a proton beam, but only one with an electron beam as in this case momentum transfer is relatively minor.

From Figure 3 and Table I we may easily deduce that an immediate consequence of energy deposition by a proton beam in the sub-MeV region is rapid heating and pressure build-up just below the transition zone. The thrust of the theoretical work is to predict the time scales and magnitudes of the resulting mass motions and to identify possible observable signatures in spectral lines. We must emphasize that most of the published work on the atmospheric response to energy deposition has been related to electron beams. However, certain features of the predictions may be legitimately scaled for a proton beam.

McClymont and Canfield (1984) considered the momentum deposited by an electron beam with a power law spectrum and a low-energy cut-off in the 5–20 keV range. They found that the momentum pressure dominated for only a few seconds, after which time the gas pressure due to heating dominated. (In most of the work discussed here the energy flux considered was in the region $1-10 \times 10^{10}$ erg cm^{-2} s^{-1}.) Furthermore, even when momentum pressure was important, the region where it dominated the gas pressure was extremely thin. However, for proton beams they cited work by Brown and Craig (1984) to show that significant downward motion of the atmosphere due to absorption of beam momentum would be expected to precede thermally-driven plasma motions. Red-shifted emission in a line such as Hα would be a signature of high levels of momentum deposition.

Tamres *et al.* (1986) studied momentum deposition by protons in more detail, starting with proton injection at the top of a coronal loop. They calculated results for two extreme cases, with mean proton energies of 20 keV and 27.5 MeV, respectively; in both cases a smoothed spectrum was used to avoid a discontinuity involved with invoking a low energy cut-off to a power law. They also considered a totally ionized atmosphere. Unfortunately the energy region of interest is midway between these extremes. Twenty keV protons will not penetrate to the top of

the transition zone, from, say 10 000 km in the corona; they stop in the corona. On the other hand 27.5 MeV protons lose most of their energy at too high a density to play an important role in chromospheric evaporation. A fully ionized atmosphere is appropriate for the coronal situation, irrelevant to the high energy case, but not appropriate for intermediate energies. Nevertheless, it is evident that the hydromagnetic effects of beam momentum deposition in the early phase of flares are important in the coronal part of the loop and in the upper chromosphere.

MacNeice *et al.* (1984) modelled the response of the solar atmosphere to energy deposition by an intense electron beam, starting from the top of a coronal loop at a height of 12 000 km above the photosphere. For an energy flux of 10^{11} erg cm^{-2} s^{-1} the loop was filled at supersonic speed with upflowing plasma, and the plasma temperature was found to rise $> 15 \times 10^6$ K within 10 s. They did not predict significant downward mass motion; momentum balance was achieved by a downward-moving compression wave. To study the way the atmosphere responds to different energy depositions, they divided it into two regions, of 'high' and 'low' density. In regions of high density, which are easiest to reach at the onset of the flare (Section 3.2) the energy is radiated away quickly and the temperature rise is minimal. In the upper chromosphere the density is too low for efficient radiation so the temperature rises rapidly. This feeds back to increase the fractional ionization, which exacerbates the effect.

Fisher *et al.* (1985) termed this 'explosive' evaporation and studied the conditions surrounding its occurrence. Generally they were able to reproduce and extend the results of MacNeice *et al.* (1984). They derived an energy flux threshold for explosive evaporation, and they put an upper limit of ~ 2.35 times the sound speed for the velocity of the explosively-evaporated plasma. MacNeice *et al.* showed that for energy fluxes $< 3 \times 10^9$ erg cm^{-2} s^{-1} the boundary between the 'high' and 'low' density regions was high in the chromosphere such that very little material would be evaporated. Generally speaking electron-heated atmospheres deposit the energy in the top layer, partly because of the predominance of large angle scattering in collisions of deka-keV electrons. Li *et al.* (1989) calculated that electron-heated atmospheres should always show significant blue-shifts in high temperature lines, such as Ca XIX, early in the flare. The lower the mean energy of the beam, which is equivalent to reducing the energy deposition depth, the stronger the predicted blue-shift.

Fisher (1987) studied the time scales for explosive evaporation to occur, again for an electron beam. He showed that if the risetime of the electron energy flux is longer than ~ 1 s, then the evaporation will not be explosive. Also, because it takes a finite time to build up the pressure, there should be a delay of ~ 0.4–0.7 s between the onset of the hard X-ray burst and the spectral line signatures, e.g., Hα red asymmetry, of explosive evaporation. The rate of energy deposition now becomes very important. Small energy fluxes evaporate a small amount of the top of the chromosphere, probably with relatively high blue-shift (Li *et al.*, 1989). Protons will in general deposit their energy somewhat lower in the chromosphere,

unless the spectrum is very soft. Increasing the energy flux merely evaporates the next layer. So even if there is a final, rapid rise in the energy flux to maximum, if it has been preceded by somewhat lower level fluxes, explosive evaporation will probably not occur.

Returning to the situation where there is explosive evaporation, there is a difference in the predicted outcome depending on whether the energy input is via a proton or an electron beam. For electrons, Fisher (1987) predicted that the Hα red asymmetry should appear after the hard X-ray burst. This is, of course, demanded from straightforward causality arguments. If the energy input is from a proton beam, not only should the Hα red shift signature be stronger, because of supplementation by momentum deposition, but it should be unrelated to the hard X-ray burst. This last point would also apply to blue-shifted signatures. The duration of the downflow due to explosive evaporation has been addressed by Fisher (1989) who predicted that 'easily observable downflows will exist for roughly 30 s'. Therefore longer lasting red-shifts would require momentum deposition to sustain them. There are many situations where the input conditions as calculated by Fisher (1987) will not produce explosive evaporation, and therefore the heating will produce negligible red-shifted Hα. In these situations a red-shift would need to be caused by momentum deposition. Therefore we would regard a near-ubiquitous Hα red-shift signature as evidence for proton beams.

4. Direct Evidence for Protons in Flares

4.1. High-energy protons, > 10 MeV

The direct evidence that energetic protons are present in solar flares comes from observations of gamma-ray lines. Nuclear processes and accelerated particles in flares have been reviewed by Ramaty and Murphy (1987); in some flares gamma-rays resulting from pion decay are observed. The pions are produced predominantly by protons and alpha particles in the energy range around 1 GeV nucl^{-1}. Figure 5 shows the time dependence of the 100 MeV and 4.1–6.4 MeV gamma-ray intensities following an intense flare on 3 June, 1982 at 11:42:11 UT. The 4.1–6.4 MeV band covers the strong gamma-ray emission lines from excited states of ^{12}C and ^{16}O. The intensity-time history of the two energy bands is quite different. Ramaty and Murphy interpreted this behaviour as indicating two different proton populations with different energy spectra. What is clear is that relativistic protons were interacting in the atmosphere for over 10 min following the flare onset. Frequently in flares the intensity-time histories of the various energy emissions is complex and reliable correlations are difficult. However, occasionally they are unambiguous. In an event on 8 February, 1982 bursts of photons from $\sim$ 40 keV–$\sim$ 40 MeV (the highest energy channel) were coincident to $\pm$1 s (Kane *et al.*, 1986). If the highest energy photons are from pion decay this would prove that a very fast acceleration

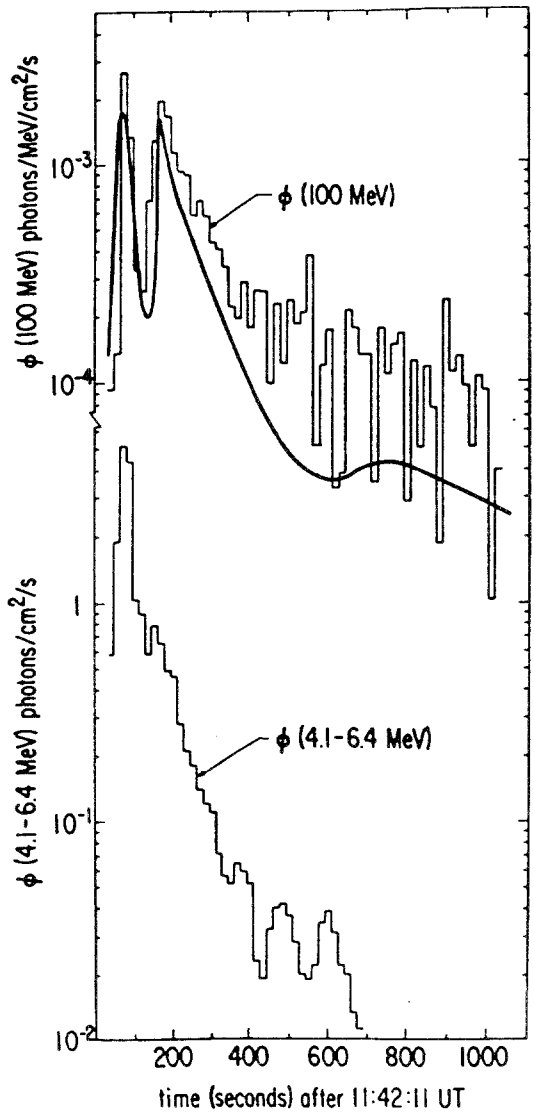

Fig. 5. The time dependence of the 100 MeV and 4.1–6.4 MeV photon intensities from the 3 June, 1982 solar flare. (After Ramaty and Murphy, 1987.)

mechanism is operating up to GeV energies, such as that discussed by Ohsawa (1985).

Flares with evidence of pion production are rare. However, on 11 and 15 June, 1991 two major events were seen from GOES Class X12 flares in AR 6659. From the 11 June flare pion decay gamma-rays were detected which were most likely caused by trapping of relativistic protons in the corona, followed by gradual loss due to pitch-angle scattering to the chromosphere (Mandzhavidze and Ramaty, 1992). Trapping for up to 8 hours is required as the gamma-ray flux took this time

to return to background levels (Kanbach *et al.*, 1993). This point is important in connection with the availability of seed particles for input to proton acceleration mechanisms.

Results from the Solar Maximum Mission (SMM) showed that gamma-ray flares were not particularly rare. Ryan and Simnett (1989) selected an optically-small gamma-ray flare for which they argued that the relative importance of the gamma-ray flux to the total flare energy was due to the re-acceleration of a seed population of protons 'left over' from a larger flare some 8 hours earlier. Thus the concept of lengthy particle trapping in the corona has direct support both from long-duration gamma-ray flares such as 11 June, 1991 and from the energetically-small, but gamma-ray rich, flares. For several large gamma-ray flares Ramaty and Murphy (1987) show that above 30 MeV, for the particles interacting at the Sun, the electron/proton ratio is $\sim 10^{-3}$ and certainly $< 10^{-2}$.

Several decades ago it was thought that the particle acceleration in the impulsive phase was limited to electrons up to 10^2 keV and that the energetic ions and highly relativistic electrons were accelerated by a second stage process generally associated with the passage of a flare-induced shock outwards through the corona. However, the gamma-ray line and neutron observations of Forrest and Chupp (1983) showed for the first time that relativistic protons were present in some flares at the onset of the impulsive phase. It is now generally accepted that there is no *fundamental* requirement for a two-stage acceleration process, although this does not preclude multiple periods of acceleration in some flares, which could have different spectra.

4.2. Low energy protons, < 1 MeV

The nuclear interactions of energetic protons give the most unambiguous evidence for their presence; they also give a physical insight into the atmospheric composition. However, because of the steep energy spectrum above 30 MeV, which is inferred from direct measurement of the particles which escape into the interplanetary medium, such protons are insignificant energetically to the total energy budget of a flare. It is difficult to extrapolate the spectrum deduced at high energies reliably into the sub-MeV region. Yet it is in the 0.1–1 MeV region that the bulk of the energy is believed to reside (Simnett, 1986). In flares, protons below the gamma-ray production threshold cannot be positively identified from observations of the intensity of emitted solar radiation. This does not mean that the low energy component does not exist, merely that we must be ingenious in devising ways to detect it. The search until recently has been elusive, but there are now promising developments in both observations of linear polarization of the Hα line and of red-shifted Lα.

4.2.1. *Linear polarization of the Hα line*

Hénoux *et al.* (1990) have reported results of polarization measurements made on the Hα line for three chromospheric flares. A half-wave plate was rotated in 22.5° steps in front of the linear polarizer of the Hα patrol heliograph at the Paris Observatory such that a set of 16 images was obtained once per minute. Subsequent analysis enabled the polarization fraction and the azimuthal direction of the polarization vector to be obtained with one minute time resolution. Figure 6 shows their result for the brightest (in soft X-rays) of the three flares. In this figure the brightest Hα regions are shown stippled. Single arrows indicate the direction of the polarization vector in the flaring regions while the double arrow shows the direction towards disk centre. The polarization is observed during the rise to maximum of the soft X-ray emission but it is not well correlated with hard X-ray emission. The polarization disappears near the time of maximum of the soft X-rays, suggesting that energy input to the flare plasma had ceased. Hénoux *et al.* argued that the polarization could not be from the Zeeman effect as in this case the polarization vector should reflect the fan shape of the sunspot magnetic field. They also showed that polarization due to the Stark effect was negligible. Consequently the remaining candidate is impact polarization from protons $\sim$ 100 keV, as discussed in Section 3.3.

Metcalf *et al.* (1992, 1994) have used the Imaging Vector Magnetograph at the University of Hawaii to measure the extent of linear polarization of the Hα line. Their instrument is considerably more sensitive than that of Hénoux *et al.* (1990) and has a time resolution of 16s. Significant linear polarization was detected from flares in October, 1992 and results from one of these are summarized in Figure 7 (Metcalf *et al.*, 1994). Figure 7(a) shows the polarization image at 00:58:51 UT on 23 October, 1992 at the peak of the 25–100 keV hard X-ray burst (Compton Gamma-ray Observatory; BATSE) which is shown in Figure 7(c). The arrow indicates the projected direction of disk centre. The background image is the Hα intensity. The polarization in the two main Hα kernels is in a direction close to that of disk centre. Figure 7(d) shows a polar diagram of the polarization vector for all pixels above a polarization threshold of 3%. Note that as the sign of the polarization vector is not determined the polar diagram is necessarily symmetrical about the E–W line. The dashed line at ESE is the direction of disk centre. Figure 7(b) shows the image at 01:02:10 UT after the decay of the hard X-ray burst. There is still a polarization signal from the main Hα kernel but more significant is the strong signal from a diffuse region in the eastern part of the image.

The polarization is almost certainly caused by sub-MeV protons moving downwards to the chromosphere along magnetic field lines inclined around 20° to the vertical. During flare maximum the proton energy spectrum and energy flux are such that hot Hα kernels and X-rays are also produced. Later in the flare there is still energy input to the chromosphere but the energy flux is now insufficient either to heat the plasma to X-ray-emitting temperatures or to generate the electrons needed for hard X-ray production (Section 2.3). During this late phase the

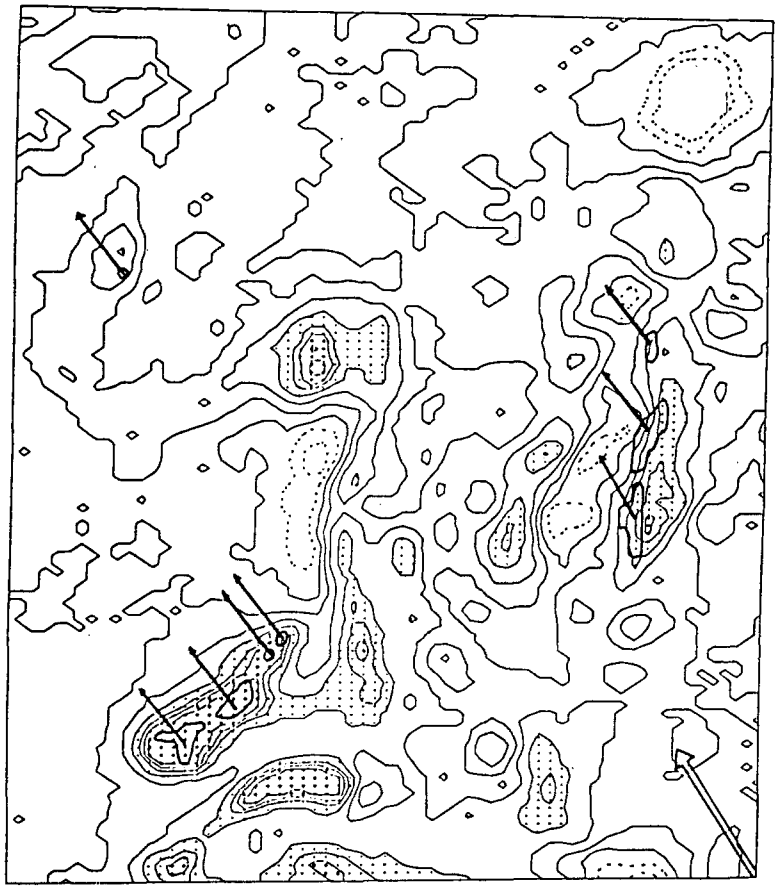

Fig. 6. An Hα filtergram showing chromospheric brightening for a solar flare on 11 July, 1982. The size of the image is $3' \times 3.3'$, with a pixel size of $3'' \times 3''$. The direction of the polarization of the electric vector is shown as single line arrows while the flare to disk centre direction is shown as a double arrow. (After Hénoux *et al.*, 1990.)

protons are probably diverted from the primary flare site, i.e., the location of the bright Hα kernels in Figure 7(a), to a more easterly location. This is consistent with interpretation of other flares by Simnett *et al.* (1990) who suggested that the output of the coronal acceleration region could be variously diverted via coronal magnetic fields to different parts of the active region. Changes in pressure in coronal loops due to explosive chromospheric evaporation (Section 3.4) could be responsible for the diversions; alternatively delayed deposition of protons accelerated during the impulsive phase, following storage in high coronal loops, could be invoked. Martens *et al.* (1990) have also studied delayed remote flare brightenings, except that they attributed them to a change in the location of the coronal reconnection site. However, both interpretations require a change in the magnetic topology in the corona during the flare.

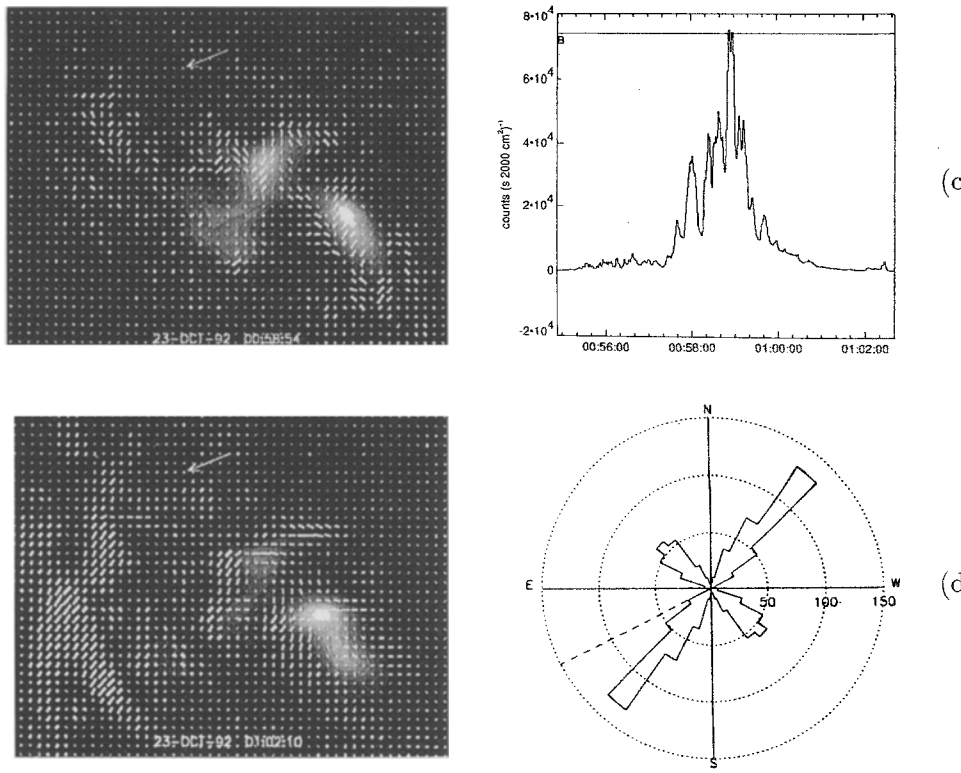

Fig. 7. (a) The underlying image is the Hα flare at 00:58:51 UT on 23 October, 1992; the matrix of short line segments shows the magnitude and direction of the linear polarization and the arrow shows the direction towards disk center. The line segments are ~ 1800 km apart on the Sun. (b) The same, only at 01:02:06 UT; note the strong polarization well away from the dominant Hα site. (c) The intensity-time history of 25–100 keV X-rays for this flare. (d) A polar histogram of Imaging Vector Magnetogram pixels with linear polarizaton in each direction at the time of the peak in the X-ray intensity (00:58:51 UT). Only pixels with linear polarization above 3% are plotted. The radial dashed line shows the direction of disk center. (After Metcalf *et al.*, 1994.)

The detection in Figure 7(b) of a strong polarization signal without a large energy flux suggests a proton spectrum which does not extend much above 100–200 keV. In fact, the energy spectrum may well be peaked in this region (see also Section 4.4), with the decrease at high energy reflecting the acceleration process and that at low energies caused by absorption and scattering in the corona. Note that the column depth of the transition region from the corona is likely to be 3×10^{18} – a few $\times 10^{19}$ cm^{-2}, which will easily stop protons of 30 keV (Table I).

Saar *et al.* (1994) have detected a rapid change in the polarization amplitude and direction over a two-hour period from the flare star BD+26°730. In trying to interpret the data several possible explanations were considered. These included rotational modulation, modulation by a companion, magnetic flux changes and impact polarization. They concluded that impact polarization caused by flare-

generated proton beams striking the chromosphere and photosphere was the most probable explanation for the observations. Furthermore they were able to estimate the energy flux to be in the range 10^9–10^{10} erg cm^{-2} s^{-1}, which is similar to some of the energy fluxes considered in Section 3.4.

In summary, the recent high-resolution Hα polarization measurements from the Sun give an unambiguous signature of sub-MeV protons in the chromosphere both in association with hard X-ray emission and in its absence. It will be important to build up the data-base in this area, preferably with complementary soft X-ray and hard X-ray images, to enable a full interpretation of the physical situation.

4.2.2. *Detection of the Red-Wing of Lα*

The polarization measurements described in the previous section rely on observations with good spatial resolution. In situations where good spatial resolution is not possible, the most sensitive diagnostic of protons in the sub-MeV energy range is red-shifted Lα emission as discussed in Section 3.2. This, unfortunately, has never been applied successfully to solar observations, for although the Ultraviolet Spectrometer and Polarimeter on SMM was designed with a suitable capability its response degraded before definitive measurements were undertaken. Canfield and Cook (1978) attempted to look for the signature in *Skylab* data, but were unsuccessful. However, the *Skylab* data had very poor time resolution and Brosius *et al.* (1994) have shown that the signature would not be expected to persist for very long (Section 3.2). Therefore the null result is not surprising.

The Goddard High Resolution Spectrograph on the Hubble Space Telescope has been used by Woodgate *et al.* (1992) to search for a Lα red-wing enhancement during a flare from the red dwarf star AU Microscopii. They found an event lasting 3 s, shown in Figure 8, which they attributed to a low energy proton beam; this occurred a few seconds after the start of the observation. Figure 8(b) shows a comparison of the red-wing (stars) with the blue-wing (diamonds). The intensity-time history of the Si III line is shown in Figure 8(c). The important next question is whether or not the energy in the protons made a significant contribution to the energy budget? Woodgate *et al.* used the predictions of Canfield and Chang (1985) to derive an integrated beam power of $> 10^{30}$ erg s^{-1} from the strength of the Lα red-wing flux. They estimated the flare energy using their simultaneous observations of the Si III line. If AU Microscopii has an elemental abundance similar to the Sun, they calculated that the total energy radiated by the plasma from which the Si III line originated was 6×10^{28} erg s^{-1}. Although there were considerable systemmatic uncertainties involved in arriving at these estimates, it is evident that taking the measurements at face value, this flare was consistent with a dominant energy input from a low-energy proton beam. It remains to be seen if these signatures are found in other stellar, or solar, flares.

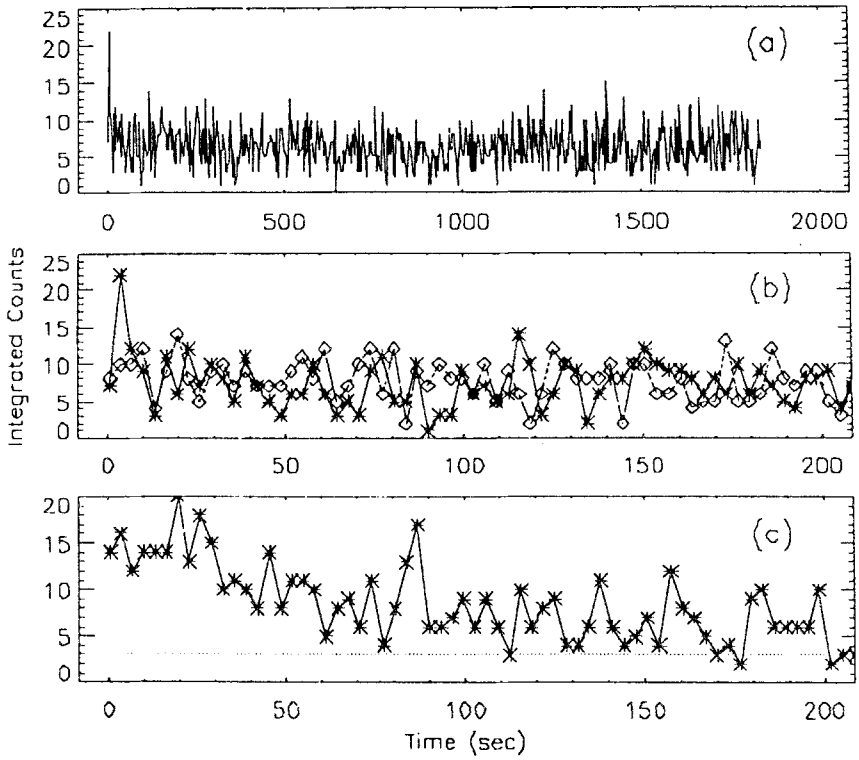

Fig. 8. (a) The intensity-time history of the Lα red-wing for a flare from AU Microscopii on 3 September, 1991. (b) A comparison of the first 200 s of (a) for the red-wing (stars) and the blue wing (diamonds). (c) The intensity-time history of the Si III line. (After Woodgate *et al.*, 1992.)

4.2.3. *Radio Observations*

Particle beams in the solar atmosphere emit radio waves at the local plasma frequency and/or its harmonic. The most commonly observed particle beam is one of mildly relativistic electrons – in a typical velocity range 0.1–0.4c, where c is the velocity of light – which produce type III radio bursts. The velocity of the exciting particles is determined from the rate at which the frequency drifts; for this one also needs a density-height model for the solar atmosphere. The plasma emission is through growing Langmuir waves, produced by the anomalous velocity distribution of the electron beam, which in a section of the high velocity region of the spectrum has a positive slope (bump-in-the-tail).

Some bursts have very slow drift rates and cannot be interpreted as due to electron beams (Benz and Simnett, 1986). Very slow drift rates imply low velocities for the exciting disturbance. One such burst discussed by Benz and Simnett corresponded to a beam velocity of only 13 000 km s^{-1}, less than double the mean thermal electron speed in the low corona. Electron beams of such low velocity cannot produce type III bursts (a) because Landau damping inhibits the growth of

Langmuir waves for velocities below about four times thermal and (b) the beam would tend towards isotropy through collisions in a time $\ll 1$ s for a source density of 3×10^8 cm^{-3}, typical of the low corona where the bursts originate. As the reported burst lasted up to 3.5 s, Benz and Simnett attributed it to a proton beam with energy in the region 0.56–3.7 MeV. They advocated that the radio emission was produced via coupling of low-frequency ion-acoustic waves generated by the proton beam with weak Langmuir waves associated with the electron current which accompanies a freely-streaming proton beam. Benz and Zlobec (1978) had previously found 34 events with very slow drift rates so this signature of proton beams is not that uncommon.

4.3. Chromospheric Evaporation and Mass Motions

We are including chromospheric evaporation as evidence for substantial energy deposition by protons, even though for many years (including the present time) its advocates have regarded it as induced by electrons. We have reviewed some of the theoretical work in Section 3.4 and many of the results of the theory relate to energy deposition at certain depths in the chromosphere with a range of energy fluxes. Whether the energy deposition is by non-thermal electrons or protons is often immaterial. The primary evidence for regarding chromospheric evaporation as proton-induced comes from the fact that in some large flares the onset of the upflows precedes the onset of the hard X-ray burst and that the flows often appear to be unaffected by rapid, major changes in the power of the hard X-ray burst. Theory (MacNeice *et al.*, 1984; Fisher *et al.*, 1985) predicts that explosive evaporation of large amounts of mass will occur if the energy flux is high, which is also likely to be the condition for producing the hard X-ray burst (Simnett and Haines, 1990). Inevitably the two phenomena should have a relatively strong correlation. If the energy flux is carried by electron beams then hard X-rays *must* be produced during the time taken to build up pressure to drive the upflow, and therefore the onset of the hard X-ray burst must, from causality arguments, always *precede* the onset of the upflow. It is reasonable to take the view (Occam's razor) that the underlying physical processes and initiating disturbances are similar for all flares. Therefore if a significant number of cases of strong upflows are found which violate the electron beam hypothesis, but can be explained by proton beams, then it would be perverse not to invoke proton beams as the origin of all strong, high temperature upflows.

Chromospheric evaporation was a controversial topic until the observations of Doschek *et al.* (1980) and Antonucci *et al.* (1982, 1984) showed conclusively that there is a blue-shift in the spectra of He-like ions, e.g., Ca XIX, Fe XXV, at the onset of many large flares. There is also substantial broadening in the resonance lines themselves. As the location of the parent flare moves towards the limb the blue-shifted component diminishes to ~zero but the line broadening remains. Therefore the blue-shift is unambiguously identified as emission from upward-moving material. The two examples we present below have been selected because

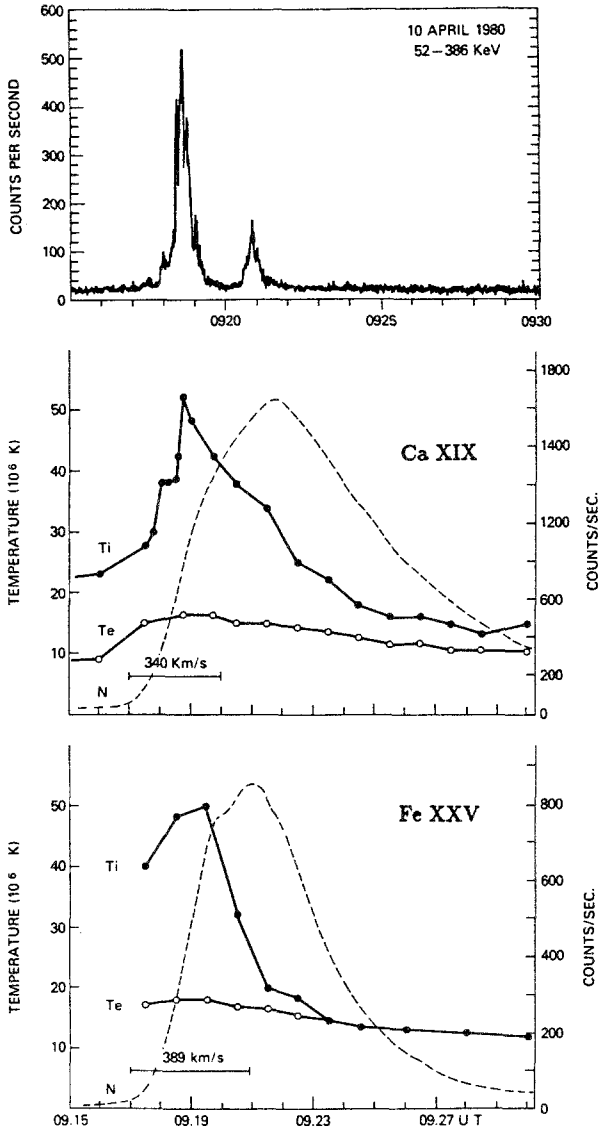

Fig. 9. *Upper panel*: the 52–386 keV X-ray intensity during the 10 April, 1980 flare. *Middle panel*: the intensity-time profile of the soft X-ray emission N integrated over the spectral region of the Ca XIX resonance line plus satellites (right scale) and the evolution of the electron temperature T_e and the equivalent ion temperature T_i. The period in which upward velocities are measured is indicated by the horizontal bar, together with the highest value of the velocity. *Lower panel*: the same, only for the Fe XXV spectrum. (After Antonucci *et al.*, 1982.)

they clearly violate the electron beam hypothesis. There are many other examples and the reader is urged to study the cited papers in this section critically to assess independently the generality of the arguments.

Antonucci *et al.* (1982, 1984) discuss large flares observed by SMM where in some instances the onset of the upflows deduced from asymmetries in the Ca XIX and Fe XXV lines clearly preceded the onset of the hard X-ray burst. Figure 9 gives a good example of this from the April 10, 1980 class M4 flare. From the Ca XIX line strong blue-shifts were observed for 3 min. The derived velocity during the first minute was 280 km s^{-1}, compared to the maximum of 340 km s^{-1} at the time of the peak in the hard X-ray burst. Similar evidence came from the Fe XXV line. The dashed lines indicate the intensity-time profile (right scale) of the X-ray emission integrated over the whole line profile. The solid lines show the evolution of the electron temperature T_e and the equivalent ion temperature T_i. The strong upflows start well before the onset of the hard X-ray burst, shown in the top panel. For this flare Antonucci *et al.* (1982) calculated that >20% of the total flare energy had already been transferred to the plasma before the onset of the hard X-ray burst. As evidence for explosive evaporation is present, this is consistent with the energy flux having exceeded $\sim 10^{10}$ erg cm^{-2} s^{-1} (MacNeice *et al.*, 1984; Fisher *et al.*, 1985) but without impulsive hard X-ray emission. Therefore this flare cannot be powered by non-thermal electron beams. This was appreciated by Antonucci *et al.* (1982) who stated: "It is difficult to conceive that an electron beam dissipating energy at the loop footpoints during the brief hard X-ray burst could maintain the evaporation process. The mechanism driving the upward motions starts before and lasts longer than the interval of maximum hard X-ray emission (20 s) during which the energy released by the electrons is relevant". They concluded that an additional energy input is needed but did not elaborate.

The *Yohkoh* satellite has a similar Bragg Crystal Spectrometer (BCS), but an order-of-magnitude more sensitive, to that flown on SMM. Thus the lack of sensitivity in the early phase of flares has been somewhat alleviated. Plunkett and Simnett (1995) examined 50 flares detected by the BCS which had simultaneous, high sensitivity, hard X-ray observations from the BATSE instrument on the Compton Gamma-Ray Observatory. Of these, 35 provided good, unambiguous coverage of the flare onset. Their results showed that in 14 flares the onset of the blue-shifted component preceded the onset of the hard X-ray burst by 15–100 s. An example of one flare, on September 6, 1992 is shown in Figure 10. Here is plotted the decrease in the first moment of the Ca XIX resonance line (thin line, left scale) and the intensity of 25–100 keV X-rays (thick line, right scale) as a function of time. A decrease in the first moment indicates the onset of a blueshift (see Mariska *et al.*, 1993 for details). The left arrow is the latest time which could possibly be assigned to the onset of the blue shift, while the right arrow is the earliest time that could be assigned to the onset of the hard X-rays. The horizontal dashed line is drawn at the time of 10% maximum of the hard X-ray intensity and the vertical dashed line is at the time of maximum decrease in the first moment.

Fludra *et al.* (1989) studied 40 flares observed with SMM of which 23 showed upflows during the impulsive phase. Of these 23, 6 showed an increase in upflow velocity at the beginning of the flare, while 'for all other flares the upflow velocity

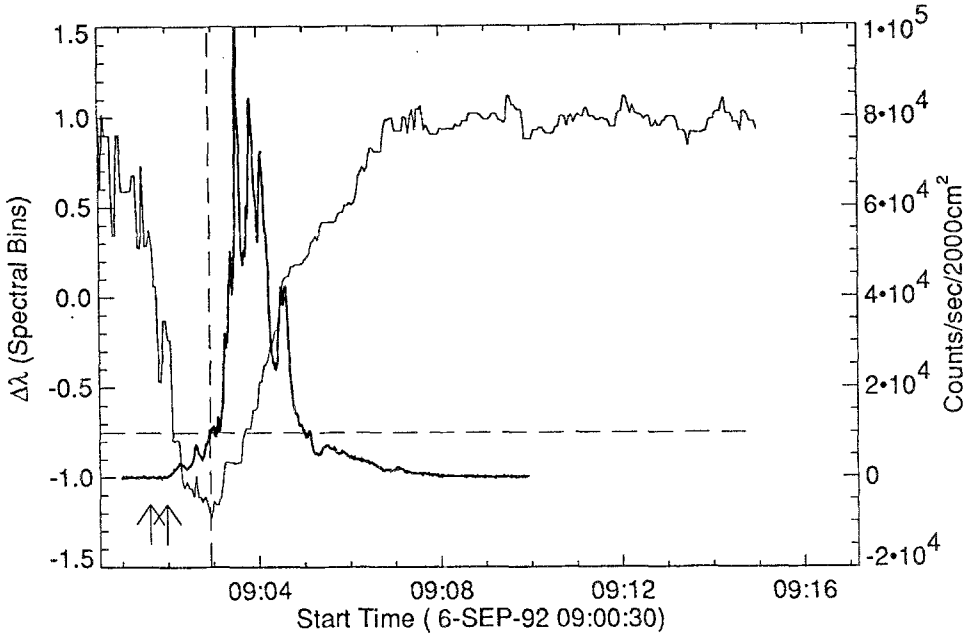

Fig. 10. The first moment of the Ca XIX resonance line (thin line) for a flare on 6 September, 1992. The 25–100 keV X-ray intensity-time profile is shown as the thick line. The left arrow indicates the latest time of onset of the blue-shifted emission, while the right arrow indicates the earliest time of onset of the hard X-rays. (After Plunkett and Simnett, 1995.)

has already reached its maximum observed value ($\sim$ 300–350 km s^{-1}) by the time the spectra have become statistically significant.' We regard the results of Fludra *et al.* (1989) as *prima facie* evidence for non-thermal protons.

Inference of other mass motions comes from spectroscopic observations of the Hα line. A red asymmetry is found during the initial phase of almost all flares that occur near disk centre (Ichimoto and Kurokawa, 1984; Tang, 1983). Ichimoto and Kurokawa showed that the red-shifted emission came from sub-arcsecond Hα kernels and that the lifetime of the emission was shorter than that of the Hα emission from the kernel. Their observations had a time resolution of 2–3 s, and at a single site the downward velocity of the mass associated with the red-shift could decrease to half its value in around 30 s. They claimed good correlation with microwave emission; however, in their published data there were also many Hα red-shifts not associated with microwave enhancements. The important features of these results have been confirmed by Canfield *et al.* (1990a) for five flares, for four of which Canfield *et al.* (1990b) demonstrated momentum balance (to within an order-of-magnitude) between upflowing and downflowing material. In two flares blue-shifted Hα emission was also seen early in the impulsive phase. Canfield and Metcalf (1987) looked for Hα red shifts associated with hard X-ray microflares and found peak downward velocities from the larger microflares of $\sim$ 100 km s^{-1}; smaller microflares showed smaller velocities. The duration of the measured red-

shifts was often over 3 min (cf., predictions of $\sim$ 30 s by Fisher (1987)) but they believed that this was due to multiple episodes of energy deposition within one pixel. They argued that the size of the emitting region was well below their spatial resolution of $\sim 3''$.

The theoretical predictions relating to explosive chromospheric evaporation are based on energy flux. For small, unresolved events it is not possible to establish the energy flux even if the total energy can be estimated. Therefore the Hα spectral studies are inconclusive regarding their support for proton beams as the red-shifts, even in small flares, could be the result of explosive evaporation from a very small area regardless of how the energy got there. However, energy deposition by proton beams should always produce a red-shift via momentum deposition, notwithstanding the production of conditions suitable for explosive evaporation. In the latter case momentum deposition will add to the pressure-induced red-shift, and thus oppositely-directed flows will be produced. On balance, we regard the almost ubiquitous Hα red-shifts as lending strong support to the proton beam hypothesis, while not providing proof.

4.4. Interplanetary Detection of Energetic Solar Protons

There are many direct observations of solar protons made either with detectors on spacecraft or by detectors on Earth. They cover the energy range from $>$ 20 GeV, the highest yet recorded, to the protons in the solar wind where the non-thermal component merges with the thermal. Proton observations by ground-based neutron monitors average little more than one/year, tending to cluster around periods when conditions on the Sun are favourable. The energy response of a ground-level monitor is governed by the atmospheric absorption (equivalent to a threshold rigidity of $\sim$ 1 GV) plus the shielding effect of the geomagnetic field, which at an equatorial location such as Darwin, Australia, is equivalent to $\sim$ 14 GV. Higher thresholds are obtained from underground monitors. The highest energy event in recent times was on 29 September, 1989 which was reliably estimated to have had protons up to 25 GeV (Swinson and Shea, 1990). This was a real limit as underground monitors with a threshold of 30 GeV saw no increase. This was the highest energy event since 25 February, 1956 which produced protons of similar energy. In both these events the protons arrived promptly so that there was no doubt that they were accelerated during the impulsive phase.

Occasionally solar conditions are exceptionally favourable for proton acceleration. In October 1989 another major proton event occurred, with slightly lower maximum energy, where the proton fluence above 10 MeV exceeded the total fluence ($>$ 10 MeV) from either of the two previous solar cycles (Shea, 1990). It has become apparent from low energy (1 MeV) interplanetary proton observations (Roelof *et al.*, 1992; 1995) that the inner heliosphere can act as a reservoir for solar flare protons which can take over a month to deplete. Therefore the exceptional fluence from the October 1989 event may well have been the result of re-acceleration

of the remnants of the giant 29 September, 1989 event. If this is true then part of the storage region is likely to be in the high corona, lower than the solar wind source surface. This should be a consideration for solar proton acceleration models.

Proton events $\ll$ 1 GeV are detected relatively frequently. In 1980, at solar maximum, Evanson *et al.* (1984) detected 49 events with energies above 45 MeV. The probability of occurrence roughly follows the solar cycle. However, as the energy decreases below $\sim$ 50 MeV the situation becomes complicated by the fact that proton fluxes in interplanetary space may come directly from a solar flare, or they might be modified, or partially accelerated, in strong interplanetary shocks. At 1 MeV it is extremely difficult to say with confidence that the observed proton fluxes in space come directly from a flare (in that they belong to the same population that interacts with the chromosphere) or if they are accelerated by an interplanetary shock.

For the study of solar flares it is only useful to measure solar particles in interplanetary space if they can be related to the parent population at the Sun. Unravelling propagation and release profiles is extremely difficult, especially at low energies. Above 30 MeV Ramaty and Murphy (1987, their Table III) summarise the escape probabilities for 11 major flares observed since 1972; there were 10 similar flares for which reliable estimates could not be made. For many flares the number of protons interacting at the Sun appears to be much greater than the number escaping, often by over an order-of-magnitude. There are three relevant parameters important to the current topic: (1) the highest energy, which can give important information on the acceleration process; (2) the shape of the low-energy spectrum, as for a spectral form given by Equation (1), with $\gamma > 2$, the energy resides at the low energy part of the spectrum (and therefore the spectrum must flatten at some point); and (3) the electron/proton ratio.

From interplanetary observations in the ecliptic plane the proton energy spectrum often flattens to give $\gamma < 2$ below 250 keV (Van Nes *et al.*, 1984), although their measurements were associated with interplanetary shocks. Therefore it is questionable as to what the true solar spectrum is. Recently the Ulysses spacecraft has been making observations at high heliographic latitudes, well away from the heliospheric current sheet. Armstrong *et al.* (1994) have reported an event on 13 June, 1993, seen at 32° S latitude, where the source had a spectrum which peaked around 270 keV, and from the pitch angle distribution appeared to have been injected from the corona. The ion spectra (predominantly protons) are shown in Figure 11. If the outwardly-streaming spectrum is truly representative of that found at the Sun, then it shows that sub-MeV protons are energetically dominant.

The electrons have relevance to our overall understanding of flares. In space, solar electrons do not exceed energies $\sim$ 100 MeV. It is clear from Figure 5 that in major flares, electrons in this general energy range must be produced via interactions of relativistic protons when the latter are present, so there is currently no evidence whatsoever that an *acceleration process* produces electrons of this energy. At the somewhat lower energy of 25–40 MeV Evanson *et al.* (1984)

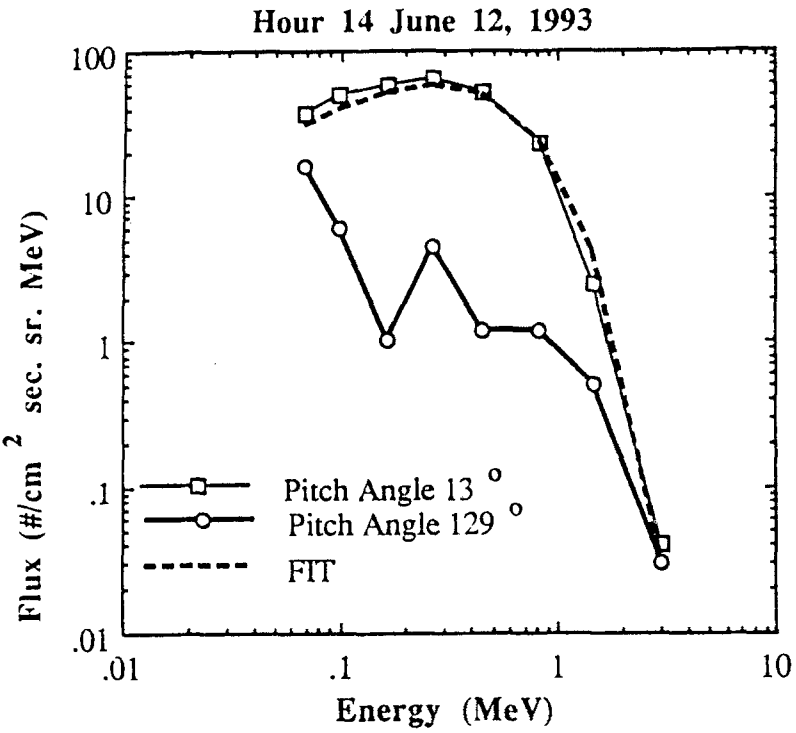

Fig. 11. Differential energy spectra of ions moving at 13° and 129° to the interplanetary magnetic field for the period 11:45–15:15 UT on 12 June, 1993. The dashed line is a Maxwellian fit with a characteristic energy of 0.273 MeV. This is interpreted as a beam of particles injected from the corona into the interplanetary medium, which are propagating with negligible scattering. (After Armstrong *et al.*, 1994.)

surveyed all particle events seen by ISEE-3 in 1980. Although the electron/proton ratio was highly variable, it had a median value of 10^{-3}, consistent with an earlier study by Datlowe (1971). All events with $e/p > 3.5 \times 10^{-3}$ ('electron rich') were from flares between W12 and W90 solar longitude, so good magnetic field connection from the spacecraft to the source is clearly important for the electrons. For a solar wind speed of 400 km s^{-1} the Earth is magnetically connected to W50 solar longitude. The electron-rich events in 1980 were also strong gamma-ray events. Although Evanson *et al.* concluded that it was the gamma-ray association that made the events electron rich, it could be partly a propagation effect. We note the review by Ramaty and Murphy (1987) who derive an e/p ratio of $\sim 10^{-3}$ in the interaction region on the Sun for several large gamma-ray flares.

In summary, interplanetary observations yield the following information on escaping solar particles:

(1) The highest energy protons ever seen (but rarely) are $\sim$ 25 GeV.

(2) The highest energy electrons are $\sim$ 100 MeV, but they may be secondary.

(3) The electron/proton ratio is $\sim 10^{-3}$.

(4) The bulk of the energy in the proton spectrum is very likely in the 0.1–1 MeV range.

5. Reconciliation of the Observations with the Expectations

We discussed in Section 3 some theoretical predictions related to the identification of non-thermal protons in the solar atmosphere, and in Section 4 we presented observations which show that protons are indeed present. However, as mentioned in the introduction, one of the main reasons for examining the role of protons in flares is to try to resolve the fundamental question as to whether protons, electrons or some collective energy dissipation, e.g., Joule heating, is the dominant energy transfer mechanism from the magnetic field to the flare. It is generally believed that this question may be simplified to one of 'protons or electrons'?

5.1. High energies

Above 30 MeV the observations of the electron/proton ratio in space are broadly consistent with those calculated on the basis of gamma-ray line and gamma-ray continuum observations from major flares. In this energy region protons are dominant, but they contain a small fraction of the total energy budget for a flare. Therefore at best the high energy observations can provide circumstantial support for the dominance of protons at low energies, through extrapolation of the spectrum.

5.2. Flare energetics

The initial controversy between electrons and protons centred on the flare energy budget. It was noted by Lin and Hudson (1976) and many others since, that a substantial amount of energy was contained in the electron population which produced the impulsive hard X-ray burst if the mechanism was non-thermal bremsstrahlung. X-ray observations can be 'inverted' to predict the electron spectrum responsible for their production and these result in steep power laws. Typically an artificial cut-off around 20 keV must be invoked to avoid exceeding the estimated total flare energy budget just in the electrons. Antonucci *et al.* (1984), while considering flare energetics associated with hard X-rays and chromospheric evaporation concluded that 'No significant additional energy input' (other than electrons > 25 keV) 'needs to be invoked, either in the impulsive phase or in the decay phase'. There is no justification for this cut-off and observations in space (Potter, 1980) have shown electron spectra extending smoothly down to the limit of the observations at 2 keV. This last observation is somewhat surprising on any model and probably should receive more attention.

We pointed out in Section 2 that most proposed acceleration mechanisms put far more energy into protons than electrons. Therefore the primary electron hypothesis has a real problem regarding acceleration of the non-thermal electrons if they

are to be dominant energetically. Smith (1985) examined electron acceleration specifically and concluded that the maximum efficiency with which energy can be transferred to streaming electrons is 23%. This limit is very convincing.

If a power law spectrum (Equation (1)) with $\gamma = 4.5$ is extended from 25–10 keV an order-of-magnitude is added to the energy. With simple equipartition between electrons and protons (recall that observations give an electron/proton ratio nearer 10^{-3}) there is a conservative 2 orders-of-magnitude oversubscription between the calculated energy and that observed. To alleviate this discrepancy we may use one of the mechanisms discussed in Section 2 and let the non-thermal electrons be produced via a secondary process. Simnett and Haines (1990) discussed one physically-plausible mechanism; there may be better ones. Simnett and Haines proposed that the non-thermal electrons were all run-away electrons accelerated in DC electric fields produced in the chromosphere by intense energy fluxes of sub-MeV protons. A low-energy cut-off appears naturally, but not necessarily at 25 keV. As discussed in Section 2.3, the energy transfer efficiency is high. The run-away electrons are in a very hot target, heated by the proton beam before the energy flux reached the critical value, and this improves the X-ray production efficiency. While this suggestion does not offer a rigorous solution to the problem, some mechanism whereby the non-thermal electrons are secondary to the protons seems the only way of solving the problem with the energy budget.

Over the last few years there has been an increasing awareness of the need for a DC electric field to provide the high energy electrons seen in flares. Holman (1985) has suggested that Joule heating by fluid aligned currents will result in the establishment of a DC electric field which will eventually lead to runaway electron acceleration. Holman and Benka (1992) applied the model to X-ray observations and showed that the energy flux in non-thermal electrons was ~ 30 times smaller than that required by classical non-thermal bremsstrahlung. Zarro *et al.* (1994) have attempted to apply this model to the flare shown in Figure 10, where there is clear evidence of energy deposition in the chromosphere early in the flare. Holman (1985) has the Joule heating in a current sheet of dimensions $10^5 \times 10^5$ km, which is necessarily in the corona. Yet the heating that occurs prior to chromospheric evaporation is in the chromosphere (Sections 3.4 and 4.3). Therefore the model as outlined by Holman (1985) while containing the very attractive feature of DC electric field acceleration, with the above-mentioned advantages to the energy budget, does not have general applicability to large flares. It also does not accelerate protons.

5.3. UV BRIGHTENINGS

In many flares there are UV brightenings without hard X-rays (Cheng *et al.*, 1984). In others, e.g., 12 November, 1980 (Cheng *et al.*, 1985) the O V emission rises several minutes before the impulsive X-rays and is relatively unaffected by their production. The O V line is produced in the transition region and it is easy to heat

that part of the atmosphere with a low energy proton beam without producing X-rays. If the hard X-rays are produced, via accelerated electrons, when the proton energy flux exceeds a critical value (Simnett and Haines, 1990) the change in power input to the transition region does not have to be affected significantly.

Orwig and Woodgate (1986) have shown that fluctuations in hard X-rays and the UV (line+continuum) can be coincident to better than 0.1 s, which was the limit of their time resolution. As Orwig and Woodgate pointed out, this cannot be achieved with an electron beam in the 20–100 keV region (deduced from the electron spectrum) as such a beam cannot penetrate to densities $\sim 10^{14}$ cm^{-3} where the UV continuum is believed to originate; MeV protons can.

5.4. Hard X-ray – soft X-ray correlation

Feldman *et al.* (1982) and Simnett (1991b) pointed out that it is impossible to predict, simply from the soft X-ray intensity-time profile, when the impulsive hard X-rays will appear. This is a controversial point, as Dennis and Zarro (1993) have argued that there is a good correlation between features in the hard X-ray burst and the time derivative of the soft X-rays. The differences between these viewpoints appears to be one of degree; correlations to $\pm$20s were required by Dennis and Zarro, while a much tighter limit was required by Simnett (1991b). With the electron beam model, a fairly precise correlation is required, especially for small, simple flares where the spatially-integrated soft X-ray light curve is not confused by long-lasting emission from a part of the flare region remote from the current hard X-ray production site. The lack of a *precise* correlation would be predicted by the Simnett and Haines (1990) model.

5.5. Rapid fluctuations in hard X-rays

Hard X-ray fluctuations on scales of $\sim$ 20 ms have been observed (Kiplinger *et al.*, 1983). Such fluctuations are difficult to achieve with an electron beam accelerated in the corona, even if the acceleration is instantaneous, due to velocity dispersion, scattering and pitch angle effects. If the electrons are accelerated in the chromosphere, rapid fluctuations are easier to achieve.

5.6. Microwave and hard X-ray delays

The delay of the microwave burst with respect to the correlated hard X-ray burst has been known for many years. It appears to vary from flare to flare. Cornell *et al.* (1984) found, from cross-correlation of five flares, a typical delay of $\sim$ 0.2 s. Costa *et al.* (1984) made the strong statement: 'no burst has yet been observed for which the microwave emission precedes the X-ray emission'. Gudel *et al.* (1991) studied the association of 20–200 ms radio spikes (in the frequency range 100–1000 MHz) with hard X-ray (25–438 keV) bursts from SMM. They found that the radio emission was usually delayed with respect to the X-rays by a few seconds. A

similar study at slightly different energies (Aschwanden *et al.*, 1993a) observed a delay of 5.16 s between the cross-correlated hard X-rays and the radio flux. A later study using BATSE hard X-ray data for two flares in September 1992 (Aschwanden *et al.*, 1993b) revealed a delay of 0.27 s.

If the X-ray emitting electrons are produced in the chromosphere via the interaction of a proton beam the delay follows quite naturally from simple causality arguments. Different delays simply reflect the time taken, with a given magnetic topology, for some of the electron population to develop into a distribution that can emit the radio signature. Starting with an electron beam in the corona, it is a triumph of ingenuity to *always* delay the radio emission from the X-rays, when simplistically it should be the converse!

5.7. Directivity of Hard X-Ray Emission

Li *et al.* (1994) have made stereoscopic observations of flares using SMM and Venera 13 and 14 data. The energy range covered was from 50–500 keV. Their results, which covered flares from essentially all longitudes, were consistent with isotropy for the emitted X-rays, showing that the electrons responsible for the emission were not beamed. This is consistent with the acceleration of the electrons in the chromosphere.

5.8. Summary

In this section we have noted that there is general consistency between proton-induced radiation at the Sun and proton detection in interplanetary space. At low energies direct proton observations cannot be correlated reliably with specific solar events due to uncertainties in propagation and interplanetary shock acceleration, plus the relative invisibility of the protons at the Sun. Therefore we have discussed a selection of different types of observation from the perspective of justifying them with primary electrons (the non-thermal electron beam hypothesis) or secondary electrons (the proton beam hypothesis). The flare energetics argument clearly favours the latter. The production of the secondary electrons is delayed by a somewhat arbitrary time from the energy deposition in the chromosphere; for small energy depositions hard X-rays may not be produced at all. Simnett (1986, 1991b, 1992) has discussed all the above selected points, and others, in more detail. The discussion in this section has been directed towards supporting the proton beam/secondary electron hypothesis and no attempt has been made to develop contrary interpretations, some of which may be found in the cited literature.

6. Towards a More Global View

If proton acceleration is to play a central role in flare development, as this paper has argued, then it is natural to enquire what other consequences there might be.

If we adopt the premise that magnetic reconnection, with current sheet formation and proton acceleration, is occurring all the time, then we might further suppose that it is only at rather special times that we get a flare. For the latter to happen, the amount of energy released must be large and the magnetic topology in the corona must be 'appropriate'. What this means in detail must await more progress in theory. So what happens to the energy output if we do not get a flare? Several possible results come to mind. Particles may be trapped in the corona, gradually losing energy, or escaping. Those that escape into interplanetary space simply add to the general population of solar energetic particles that is ever-present. Those that escape towards the chromosphere contribute to the general heating. Could active regions represent the preferred dumping ground? There could be bursts of particles that might impact the chromosphere and Simnett (1994) suggested they might power the explosive events in the transition zone (Brueckner and Bartoe, 1983). Regarding the trapped particles, Simnett and Harrison (1985) believed that the coronal heating that they provided through Coulomb collisions could provide the trigger for the energetic phenomenon we know as a coronal mass ejection (CME).

In recognition of the need to consider the global implications of having a relatively invisible, but powerful, energy source in the non-thermal protons, we now discuss briefly their possible role in the onset of coronal mass ejections and the generation of explosive events in the transition zone.

6.1. THE ONSET OF CORONAL MASS EJECTIONS

Following studies of CMEs using the Coronagraph/Polarimeter on SMM it was realised (Wagner, 1983) that their onsets were at least several minutes prior to the associated flare. Not every CME can be identified with a flare, but some missing flares may be behind the limb. Prior to this CMEs were regarded as the response to a flare; the subsequent blast wave blew away a section of the corona. When this concept was proved incorrect it became clear for the first time that a flare was a truly secondary phenomenon to a process that was taking place remotely. It then became necessary to understand the physical processes responsible, and desirable to search for signatures, other than faint changes to photospheric light scattered in the corona, that something dramatic was about to happen.

Simnett and Harrison (1985) and Harrison *et al.* (1985) searched for X-ray signatures around the time of CMEs. They discovered weak soft X-ray enhancements, often from points separated by $\gtrsim 10^5$ km, around the projected onset time of the CME. If a subsequent flare occurred it was from a point close to, but not identical with, one of the initial bright points. An example of the phenomenon is shown in Figure 12. The impression gained from these studies was that at the onset of a CME the chromosphere was sprinkled with small energy deposits. As the CME departed, more evidence of energy deposition was seen; sometimes this was a major flare, at other times two or more small events. The CME on 10 April, 1980 departed

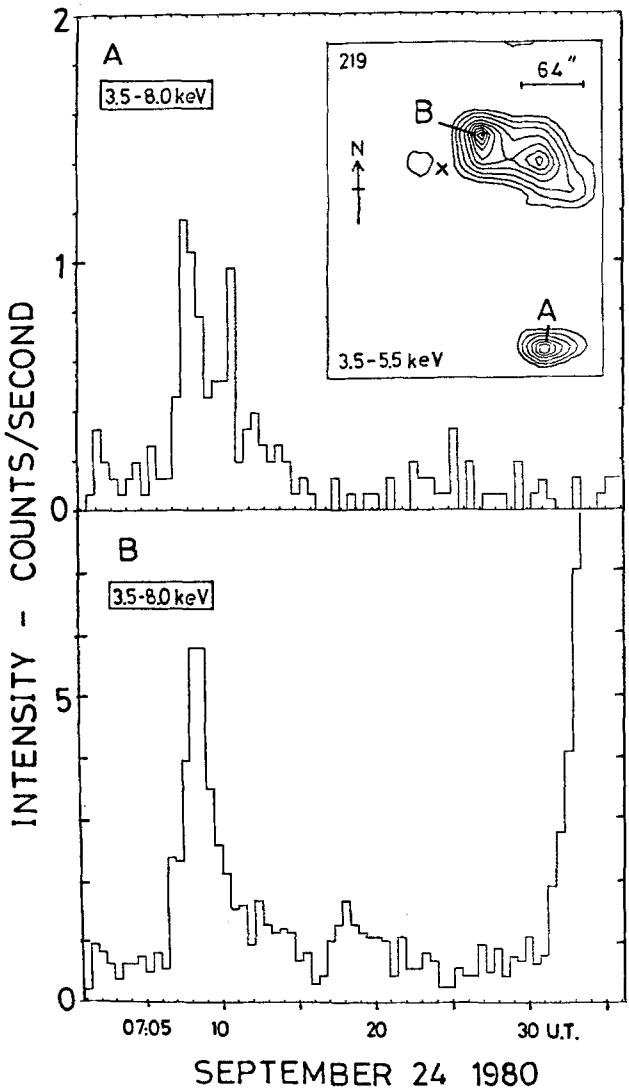

Fig. 12. The 3.5–8.0 keV X-ray activity from two widely separated points A and B from 07:01–07:36 UT on 24 September, 1980. Inset is the 3.5–5.5 keV image from 07:06:54–07:13:14 UT. The location of the subsequent flare is marked with an ×. (After Simnett and Harrison, 1985.)

over the solar north pole and as it left there was a small X-ray event from the west limb plus a precisely coincident Hα sub-flare, both in onset and decay, from N16 E32.

Simnett and Harrison (1985) suggested that protons in the 10^2–10^3 keV region were responsible both for triggering the CME and for the chromospheric manifestations. If protons are injected into a coronal loop of height 10^{10} cm, and a mean density, $\bar{\rho}$, of 4×10^8 cm^{-3}, a 130 keV proton will lose its energy through Coulomb

collisions after around one traversal (depending somewhat on pitch angle). A 500 keV proton would have a lifetime of around 9 min. The energy deposited will raise the temperature of the gas in the loop. Protons in the above energy range have the potential for transferring energy to the coronal gas which is unparalleled. An energy input of 10^{27} erg is sufficient to raise the temperature of 10^{29} cm^{-3} of the corona ($\overline{\rho} \sim 4 \times 10^8$ cm^{-3}) by 10^6 K. If this process does cause the onset of CMEs, this temperature increase in a coronal loop would approximately double the pressure.

The accelerated protons which are not trapped will immediately travel along the magnetic field to the footprints of the loop where they would produce coincident soft X-ray or Hα brightenings. The departure of the CME will drive subsequent magnetic reconnection which could, if sufficient energy were involved, accelerate enough protons to power an associated flare.

6.2. Explosive Events in the Transition Zone

Explosive events in the transition zone were discovered by Brueckner and Bartoe (1983) who identified two types of event; relatively energetic blue-shifted jets and more frequent, but less energetic, events with line profiles that were more symmetrically-broadened. The events are best observed in the C IV line, but they cover emission lines formed at temperatures from 2×10^4 K to at least 2×10^5 K. They are not seen in spectral lines formed in the upper chromosphere below 2×10^4 K and therefore are a transition zone phenomenon. Simnett (1994) has suggested that they may be produced by deposition of energy from protons accelerated in the corona which have just enough energy to penetrate below the transition zone.

From the discussion in Section 6.1, protons accelerated high in the corona will not penetrate to the top of the transition zone unless their energy is above $\sim$ 100 keV; they will merely heat the corona. If we suppose a power-law size spectrum to the energy increases, and assume that the spectral form is invariant, then as we move up the energy scale we shall start to see events which, instead of heating the corona, start to dump most of their energy in the transition zone. As the energy increases further, the energy flux may exceed the threshold for explosive evaporation to occur (Section 3.4) and the blue-shifted jets are seen. Increasing the energy still further will start to heat enough material to produce a soft X-ray event, and it will, by definition, cease to be thought of as a transition zone event. Simnett and Dennis (1986) reported impulsive soft X-ray events which lasted 30–100 s, similar to the lifetimes of the explosive events. Sometimes the events had shorter duration counterparts above 30 keV, however this was not predictable simply from the intensity of the soft X-ray burst. Some discrete hard X-ray spikes last only a few seconds (Lin *et al.*, 1984).

It is interesting to see if the duration of the transition zone events could give a clue to their origin. Suppose we take the proton spectrum shown in Figure 11

as representative of the coronal source spectrum. This steepens to $\gamma > 2$ around 800 keV; therefore most of the power is below this energy. If we take the energy deposited below the transition zone as originating in the primary spectrum from 200–800 keV, the difference in proton velocities between these limits, Δv, is $\sim$ 6000 km s^{-1}. If we take a semicircular loop of apex 10^{10} cm, the distance, l, to the transition zone is $\sim \frac{1}{2}\pi \times 10^{10}$ cm. Then the duration, S, of a transition zone event caused by an injection of protons over a time $\ll S$, is $l/\Delta v \sim 25$ s. Pitch-angle effects will increase this somewhat. It is now easy to appreciate the problem caused by 20 ms X-ray intensity fluctuations identified in Section 5.4. However, we should point out that the above explanation is merely consistent with the observations, while not necessarily excluding other interpretations.

The explosive transition zone events, plus the short duration soft X-ray spikes have a natural explanation in terms of energy deposition by protons. Whether or not hard X-rays are seen is simply a question of energy flux – note: not total energy – although a high value of one probably implies a high value of the other. The transition zone events by their definition cannot contain significant energy in high-energy protons. For a canonical spectrum this means that the total energy is limited, and consequently the energy flux is likely to be small.

7. Conclusions

We have presented a contemporary view of the theory surrounding the production of energetic protons, how they propagate through the atmosphere, and the likely signatures when they interact with the chromosphere. The principal assumption is only that the energy source is in reconnecting coronal magnetic fields. The observational evidence for proton production in flares was reviewed, starting with the gamma-ray evidence and extending to the promising new Hα polarization data. In the future red-shifted Lα radiation may be detectable, as it has already been seen in a flare from AU Microscopii. Slowly-drifting type III radio bursts are probable evidence for proton beams in the low corona.

We now turn to the real reason for the interest in protons in flares, which is to reconcile all the available evidence with a consistent flare energy budget. If the conventional explanation for the production of typical hard X-ray bursts in flares is accepted, the power for the whole flare is supplied by those electrons. In Sections 4 and 5 we presented evidence in many different forms that this concept was variously impossible, improbable or doubtful.

Let us develop the energy argument in a slightly different way. It is clearly very important to have hard evidence for the non-thermal electron/proton ratio. For emissions where protons (ions) are indisputably the only conceivable source, such as gamma-ray lines, there is no escaping the fact that the electron/proton ratio is $\sim 10^{-3}$. This ratio might be stretched to 10^{-2}, but equally it could be

m_e/m_p, as predicted by some acceleration mechanisms. Interplanetary charged particle measurements are entirely consistent with these numbers.

If we extrapolate the spectra of both protons and electrons > 30 MeV down to low energies, the bulk of the energy would be in the protons, certainly if we stop at energies that can penetrate from the corona to the transition zone. The shapes of the measured electron and proton energy spectra are not sufficiently different to expect the 10^2–10^3 factor at high energies to reverse at low energies in favour of the electrons.

There is, potentially, a way out of the dilemma, for we could invoke two types of flare. 'Normal' flares, where the energy is in the electrons and 'proton' flares where, suddenly and inexplicably, proton acceleration to > 10 MeV takes over. However, it has recently been argued (Cliver *et al.*, 1994) that gamma-ray line flares are no different from other large flares without line emission, which is of course a requirement of the proton hypothesis. Figure 13 shows the correlation of the 4–8 MeV gamma-ray line fluence with the > 50 keV hard X-ray fluence. This correlation shows no evidence for two populations of flares. Crosby *et al.* (1993) presented the size spectrum of 7045 X-ray events from 1980–1982, above 25 keV (the limit of their data) and have found a $\log N - \log S$ slope of -1.73 over the full range, as shown in Figure 14. The turn-over below counting rates of 30 s^{-1} is due to the sensitivity limit of the detector. These data also strongly suggest a single distribution of flares.

Since the suggestion was advanced in the mid-1980s that protons might carry the bulk of the energy in flares, detailed modelling calculations have begun to bring out inconsistencies with the electron beam hypothesis (Peres *et al.*, 1987; Mariska and Zarro, 1991). The most attractive feature of the non-thermal proton hypothesis is that it can plausibly account for a wide range of solar phenomena simply by taking a canonical spectrum, characteristic of the fundamental acceleration process, and adjusting the axes to give flares of different energy.

The acceleration can be in reconnecting magnetic fields in the high corona, where conditions are certainly most favourable for accelerating protons to high energies (cf., 25 GeV). Although the highest energies are only rarely attained it is an advantage to invoke a mechanism whereby under certain conditions the rarity can be achieved without requiring a new model. The reconnection is occurring quasi-continuously but only occasionally to the energies become sufficient to power a flare. Some years ago Elliot (1964) advanced gradual acceleration and storage of energetic protons, average energy $\sim$ 10 MeV, as a means of powering flares. Although we have argued here that this energy is too high, some aspects of his model are worth keeping in mind.

Turning to more global phenomena, the onset of coronal mass ejections is consistent with the general idea of quasi-continuous reconnection and proton acceleration. There has been much debate about coronal heating. Parker (1988) drew attention to the role of nanoflares (equivalent to the events discussed in Section 6.2) in this process. However, he regarded nanoflares as the intermediate stage through

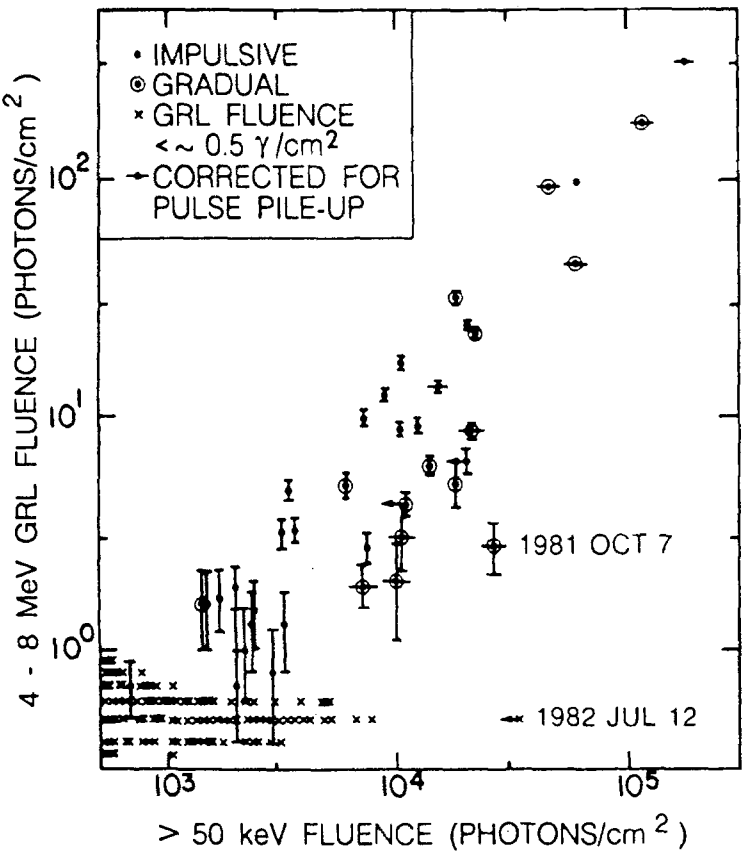

Fig. 13. The correlation between the 4–8 MeV gamma-ray line fluence and the > 50 keV X-ray fluence for flares detected by SMM from 1980–1982. Explanation of the symbols is in the inset. (After Cliver *et al.*, 1994.)

which energy was input into the corona. The energetics become rather different if the primary energy from the reconnection heats the corona via Coulomb collisions of the protons, and the nanoflares are merely a secondary phenomenon.

A way out of the apparent dilemma with the hard X-ray burst was proposed by Simnett and Haines (1990), who argued that the electrons which produce it are secondary, accelerated in the chromosphere. There may be other more appropriate models, but it is clear that the requirement that the electrons be secondary, and accelerated in the chromosphere, is valid. An important thing to recognise with a secondary phenomenon is that the energy associated with it does not have to do anything else. We do not have to look to the flare as the source of energy for the CME; we do not have to look to the electrons to provide the energy for the flare; we do not have to look to nanoflares to heat the corona. The consequences of having any of the above secondary processes regarded as primary are clear.

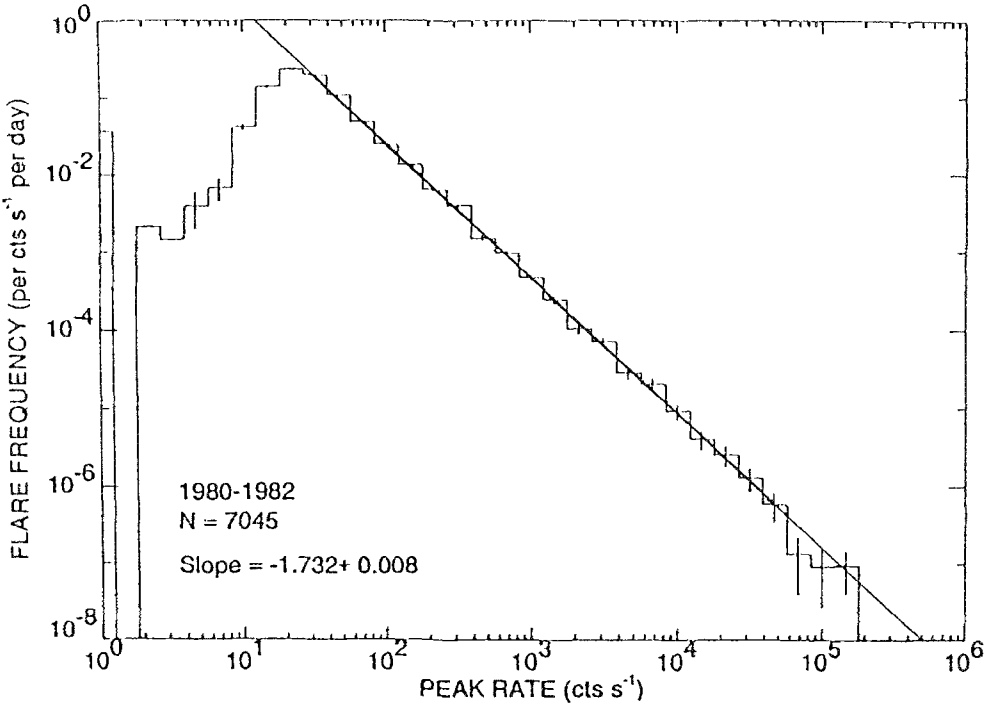

Fig. 14. The frequency distribution of the peak hard X-ray intensity > 25 keV for 7045 flares detected by SMM in 1980–1982. The turnover below 30 counts s^{-1} corresponds to the instrument sensitivity limit. (After Crosby *et al.*, 1993.)

8. Addendum: What Next?

The most promising avenue in the near future appears to lie in the high-resolution spectroscopic measurements which are possible already from the Imaging Vector Magnetograph at the University of Hawaii, plus Lα and high-resolution ion spectra which may only be taken from space. The Hubble Space Telescope, *Yohkoh* and the imminent launch of SOHO should provide ample opportunity to study the latter. More sensitive gamma-ray measurements would be able to detect lower fluxes of protons, but until a satisfactory model for the production of hard X-rays from protons has been developed, the generation of the hard X-rays will continue to be a problem. The development of a comprehensive theoretical model to investigate the behaviour of the solar atmosphere under proton bombardment does not appear practical in the short term, although that should not deter those who attempt to find a satisfactory solution to the problems discussed in this review.

Acknowledgements

I am grateful to Professor C. de Jager for inviting me to write this review. Mrs Tina Campbell was responsible for converting the handwritten text into a legible document.

References

Alfvén H. and Carlqvist, P.: 1967, *Solar Phys.* **1**, 120.
Antonucci, E., Gabriel, A. H., and Dennis, B. R.: 1984, *Astrophys. J.* **287**, 917.
Antonucci, E., Gabriel, A. H., Acton, L. W., Culhane, J. L., Doyle, J. G., Leibacher, J. W., Machado, M. E., Orwig, L. E., and Rapley, C. G.: 1982, *Solar Phys.* **78**, 107.
Armstrong, T.P., Haggerty, D., Lanzerotti, L. J., Maclennan, C. G., Roelof, E. C., Forsyth, R., Balogh, A., Pick, M., Simnett, G. M., Gold, R. E., Krimigis, S. M., Anderson, K. A., Lin, R. P., and Sarris, E. T.: 1994, *Geophys. Res. Letters* **21**, 1747.
Aschwanden, M. J., Benz, A. O., and Schwartz, R. A.: 1993a, *Astrophys. J.* **417**, 790.
Aschwanden, M. J., Benz, A. O., Dennis, B. R., and Gaizauskas, V.: 1993b, *Astrophys. J.* **416**, 857.
Benz, A. O.: 1985, *Solar Phys.* **96**, 357.
Benz, A. O. and Simnett, G. M.: 1986, *Nature* **320**, 508.
Benz, A. O. and Zlobec, P.: 1978, *Astron. Astrophys.* **63**, 137.
Brosius, J. W., Robinson, R. D., and Maran, S. P.: 1994, *Astrophys. J.* (in press).
Brown, J. C.: 1991, *Phil. Trans. Roy. Soc.* **A336**, 413.
Brown, J.C. and Craig, I.J.D.: 1984, *Astron. Astrophys.* **130**, L5.
Brueckner, G. E. and Bartoe, J-D. F.: 1983, *Astrophys. J.* **272**, 329.
Canfield, R. C. and Chang, C-R.: 1985, *Astrophys. J.* **295**, 275.
Canfield, R. C. and Cook, J. W.: 1978, *Astrophys. J.* **225**, 650.
Canfield, R. C. and Metcalf, T. R.: 1987, *Astrophys. J.* **321**, 586.
Canfield, R. C., Zarro, D. M., Metcalf, T. R., and Lemen, J. R.: 1990a, *Astrophys. J.* **348**, 333.
Canfield, R. C., Kiplinger, A. L., Penn, M. J., and Wülser, J-P.: 1990b, *Astrophys. J.* **363**, 318.
Cheng, C. C., Tandberg-Hanssen, E., and Orwig, L. E.: 1984, *Astrophys. J.* **278**, 853.
Cheng, C.-C., Pallavicini, R., Acton, L. W., and Tandberg-Hanssen, E.: 1985, *Astrophys. J.* **298**, 887.
Chiueh, T.: 1988, *Astrophys. J.* **333**, 366.
Cliver, E. W., Crosby, N. B., and Dennis, B. R.: 1994, *Astrophys. J.* **426**, 767.
Colgate, S. A.: 1978, *Astrophys. J.* **221**, 1068.
Cornell, M. E., Hurford, G. J., Kiplinger, A. L., and Dennis, B. R.: 1984, *Astrophys. J.* **279**, 875.
Costa, J. E. R., Kaufmann, P., and Takakura, T.: 1984, *Solar Phys.* **94**, 369.
Crosby, N. B., Aschwanden, M. J., and Dennis, B. R.: 1993, *Solar Phys.* **143**, 275.
Datlowe, D. W.: 1971, *Solar Phys.* **17**, 436.
De Jager, C. and de Jonge, G.: 1978, *Solar Phys.* **58**, 127.
Decker, R. B. and Vlahos, L.: 1986, *Astrophys. J.* **306**, 710.
Dennis, B. R. and Zarro, D. M.: 1993, *Solar Phys.* **146**, 177.
Doschek, G. A., Feldman, U., Kreplin, R. W., and Cohen, L.: 1980, *Astrophys. J.* **239**, 725.
Dungey, J.W.: 1953, *Phil. Mag.* **44**, 725.
Elliot, H.: 1964, *Planetary Space Sci.* **12**, 657.
Evanson, P., Meyer, P., Yanagita, S., and Forrest, D. J.: 1984, *Astrophys. J.* **283**, 439.
Feldman, U., Cheng, C. C., and Doschek, G. A.: 1982, *Astrophys. J.* **255**, 320.
Fisher, G. H.: 1989, *Astrophys. J.* **346**, 1019.
Fisher, G. H.: 1987, *Astrophys. J.* **317**, 502.
Fisher, G. H., Canfield, R. C., and McClymont, A. N.: 1985, *Astrophys. J.* **289**, 414, 425.
Fludra, A., Lemen, J. R., Jakimiec, J., Bentley, R. D., and Sylwester, J.: 1989, *Astrophys. J.* **344**, 991.
Forrest, D. J. and Chupp, E. L.: 1983, *Nature* **305**, 291.
Foukal, P., Little, R. and Gilliam, L. 1987, *Solar Phys.* **114**, 65.
Giovanelli, R. G.:, 1947, *Nature* **158**, 81.

Güdel, M., Aschwanden, M. J., and Benz, A. O.: 1991, *Astron. Astrophys.* **251**, 285.
Harrison, R. A., Waggett, P. W., Bentley, R. D., Phillips, K. J. H., Bruner, M., Dryer, M., and Simnett, G. M.: *Solar Phys.* **97**, 387.
Hénoux, J.-C. and Chambe, G.: 1990, *J. Quant. Spectr. Rad. Transfer* **44**, 193.
Hénoux, J.-C. and Semel, M.: 1981, in V. N. Obridko (ed.), *Solar Maximum Year*, Proc. Int. Workshop, Moscow, Vol. 1, p. 207.
Hénoux, J;-C., Chambe, G., Smith, D., Tamres, D., Feautrier, N., Rovira, M., and Sahal-Bréchot, S.: 1990, *Astrophys. J. Suppl.* **73**, 303.
Hénoux, J-C., Chambe, G., Semel, M., Sahal S., Woodgate B., Shine, D., Beckers, J., and Machado, M. E.: 1983, *Astrophys. J.* **265**, 1066.
Holman, G. D.: 1985, *Astrophys. J.* **293**, 584.
Holman G. D. and Benka, S. G.: 1992, *Astrophys. J.* **400**, L79.
Hoyng, P., Brown, J. C., and Van Beek, H. F.: 1976, *Solar Phys.* **48**, 197.
Hoyng, P.: 1977, *Astron. Astrophys.* **55**, 23, 31.
Hoyng, P., Duijveman, A., van Gruensven, T. F. J., and Nicholson, D. R.: *Astron. Astrophys.* **91**, 17.
Ichimoto, K. and Kurokawa, K.: 1984, *Solar Phys.* **93**, 105.
Kanbach, G. *et al.*: 1993, *Astron. Astrophys.* **272**, 744.
Kane, S. R., Chupp, E. L., Forrest, D. J., Share, G. H., Rieger, E.: 1986, *Astrophys. J.* **300**, L95.
Kiplinger, A. L., Dennis, B. R., Emslie, A. G., Frost, K. J., and Orwig, L. E.: 1983, *Astrophys. J.* **265**, L99.
Kopp, R. A. and Poletto, G.: 1986, in A. I. Poland (ed.), *Coronal and Prominence Plasmas*, NASA CP-2442, p. 469.
LaRosa, T. N. and Morre, R. L.: 1993, *Astrophys. J.* **418**, 912.
LaRosa, T. N., Morre, R. L., and Shore, S. N.: 1994, *Astrophys. J.*, submitted.
Li, P., Emslie, A. G., and Mariska, J. T.: 1989, *Astrophys. J.* **341**, 1075.
Li, P., Hurley, K., Barat, C., Niel, M., Talon, R., and Kurt, V.: 1994, *Astrophys. J.* **426**, 758.
Lin, R. P. and Hudson, H. S.: 1976, *Solar Phys.* **50**, 153.
Lin, R. P., Schwartz, R. A., Kane, S. R., Pelling, R. M., and Hurley, K. C.: 1981, *Astrophys. J.* **251**, L109.
MacNeice, P., McWhirter, R. W. P., Spicer, D. S., and Burgess, A.: 1984, *Solar Phys.* **90**, 357.
Mandzhavidze, N. and Ramaty, R.: 1992, *Astrophys. J.* **389**, 739.
Mariska, J. T. and Zarro, D. M.: 1991, *Astrophys. J.* **381**, 572.
Mariska, J. T., Doschek, G. A., and Bentley, R. D.: 1993, *Astrophys. J.* **419**, 418.
Martens, P. C. H.: 1988, *Astrophys. J.* **330**, L131.
Martens, P. C. H. and Young, A.: 1990, *Astrophys. J. Suppl.* **73**, 333.
Martens, P. C. H., Golub, L., and Herant, M.: 1990, in M. A. Dubois, F. Bely-Dubau, and D. Gresillon (eds.), 'Solar Plasma Phenomena', *Les Editions de Physique,* Les Ulis Cedex, France, p. 153.
McClymont, A. N. and Canfield, R. C.: 1984, *Astron. Astrophys.* **136**, L1.
Melrose, D. B. and McClymont, A. N.: 1987, *Solar Phys.* **113**, 241.
Metcalf, T. R., Mickey, D., Canfield, R. C., and Wülser, J.-P.: 1994, *AIP Conference Proc.* **194**, 59.
Metcalf, T. R., Wülser, J.-P., Canfield, R. C., and Hudson, H. S.: 1992, in J. Ryan and T. Vestrand (eds.), *Proc. 2nd GRO Workshop, Annapolis, MD.*
Murphy, R. J. *et al.*: 1993, *Proc 23rd Int. Cosmic Ray Conf., Calgary* **3**, 99.
Ohsawa, Y.: 1985, *Phys. Fluids* **28**, 2130.
Orrall, F. Q. and Zirker, J. B.: 1976, *Astrophys. J.* **295**, 648.
Orwig, L. E. and Woodgate, B. E.: 1986, in D. F. Neidig (ed.), *The Lower Atmosphere of Solar Flares*, p. 306.
Parker, E. N.: 1988, *Astrophys. J.* **330**, 474.
Percival, I. C. and Seaton, M. J.: 1959, *Phil. Trans. Roy. Soc. London* **A251**, 113.
Peres, G., Reale, F., Serio, S., and Pallavicini, R.: 1987, *Astrophys. J.* **312**, 895.
Peterson, B. R.: 1989, *Solar Phys.* **121**, 299.
Plunkett, S. P. and Simnett, G. M.: 1995, *Solar Phys.*, in press.
Potter, D. W.: 1981, *J. Geophys. Res.* **86**, 11111.
Ramaty, R. and Murphy, R.J.: 1987, 45, 213.
Ramaty, R., Kozlovsky, B., and Lingenfelter, R. E.: 1979, *Astrophys. J. Suppl.* **40**, 487.

Roelof, E. C., Gold, R. E., Simnett, G. M., Tappin, S. J., Armstrong, T. P., and Lanzerotti, L. J.: 1992, *Geophys. Res Letters* **19**, 1243.
Roelof, E. C., Simnett, G. M., and Armstrong, T. P.: 1994, *Space Sci. Rev.* **72**, 309.
Roizman, G. S. and Shevchenko, V. S.: 1982, *Soviet Astron. Letters* **8**, 85.
Ryan, J. M. and Simnett, G. M.: 1989, *Astrophys. J.* **341**, 506.
Saar, S. H., Martens, P. C. H., Huovelin, J., and Linnaluoto, S.: 1994, *Astron. Astrophys.* **286**, 194.
Sakai, J. and Ohsawa, Y.: 1987, *Space Sci. Rev.* **46**, 113.
Sakai, J., Tajima, T., Nakajima, H., Kosugi, T., Brunel, F., and Zaidman, E.: 1987, in B. R. Dennis, L. E. Orwig, and A.L. Kiplinger (eds.), *Rapid Fluctuations in Solar Flares*, NASA CR-2449, p. 393.
Shea, M. A.: 1990, *Proc. 21st Int. Cosmic Ray Conf., Adelaide* **12**, 196.
Simnett, G. M.: 1986, *Solar Phys.* **106**, 165.
Simnett, G. M.: 1991a, *Mem. Soc. Astron. Ital.* **62**, 359.
Simnett, G. M.: 1991b, in Uchida *et al.* (eds.), *Flare Physics in Solar Activity Maximum 22, Lecture Notes in Physics* **387**, 100.
Simnett, G. M. and Dennis, B. R.: 1987, in B. R. Dennis, L. E. Orwig and A. Kiplinger (eds.), *Rapid Fluctuations in Solar Flares*, NASA CR-2449, p. 123.
Simnett, G. M.: 1994, *Space Sci. Rev.* **70**, 69.
Simnett, G. M. and Harrison, R. A.: 1985, *Solar Phys.* **99**, 291.
Simnett, G. M. and Haines, M.G.: 1990, *Solar Phys.* **130**, 253.
Simnett, G. M., Sotirovsky, P., and Simon, G.: 1990, *Astron. Astrophys.* **227**, 235.
Smith, D. F.: 1985, *Astrophys. J.* **288**, 801.
Speiser, T. W.: 1965, *J. Geophys. Res.* **70**, 4219.
Sweet, P.: 1969, *Ann. Rev. Astron. Astrophys.* **7**, 149.
Swinson, D. B. and Shea, M. A.: 1990, *Geophys. Res. Letters* **17**, 1073.
Tamres, D. H. Canfield, R. C., and McClymont, A. N.: 1984, *Astrophys. J.* **309**, 409.
Tang, F.: 1983, *Solar Phys.* **83**, 15.
Van Nes, P., Reinhard, R., Sanderson, T. R., and Wentzel, K.-P.: 1984, *J. Geophys. Res.* **89**, 2122.
Vernazza, J. E., Avrett, E. H., and Loeser, R.: 1973, *Astrophys. J.* **184**, 605.
Wagner, W. J.: 1983, *Adv. Space Res.* **2**(11), 203.
Wentzel, D. G.: 1965, *J. Geophys. Res.* **70**, 2716.
Winglee, R. M., Pritchett, P. L., and Dulk, G. A.: 1988, *Astrophys. J.* **329**, 440.
Woodgate, B. E., Robinson, R. D., Carpenter, K. G., Maran, S. P., and Shore, S. N.: 1992, *Astrophys. J.* **397**, L95.
Zaitsev, V. V. and Stepanov, A. V.: 1992, *Solar Phys.* **139**, 343.
Zarro, D. M., Mariska, J. T., and Dennis, B. R.: 1994, NASA-GSFC preprint.